2015

Global patterns and environmental controls of perchlorate and nitrate co-occurrence in arid and semi-arid environments

W. Andrew Jackson
Texas Tech University, andrew.jackson@ttu.edu

J. K. Böhlke
U.S. Geological Survey, 431 National Center, Reston, VA

Brian J. Andraski
U.S. Geological Survey, 2730 N. Deer Run Rd, Carson City, NV

Lynne Fahlquist
U.S. Geological Survey, 1505 Ferguson Ln, Austin, TX

Laura Bexfield
U.S. Geological Survey, 5338 Montgomery Blvd. NE, Suite 400, Albuquerque, NM

See next page for additional authors

Available online at www.sciencedirect.com

ScienceDirect

Geochimica et Cosmochimica Acta 164 (2015) 502–522

Geochimica et Cosmochimica Acta

www.elsevier.com/locate/gca

Global patterns and environmental controls of perchlorate and nitrate co-occurrence in arid and semi-arid environments

W. Andrew Jackson [a,*], J.K. Böhlke [b], Brian J. Andraski [c], Lynne Fahlquist [d], Laura Bexfield [e], Frank D. Eckardt [f], John B. Gates [g], Alfonso F. Davila [h], Christopher P. McKay [i], Balaji Rao [a], Ritesh Sevanthi [a], Srinath Rajagopalan [j], Nubia Estrada [a], Neil Sturchio [k], Paul B. Hatzinger [l], Todd A. Anderson [a], Greta Orris [m], Julio Betancourt [b], David Stonestrom [n], Claudio Latorre [o,p], Yanhe Li [q], Gregory J. Harvey [r]

[a] *Texas Tech University, Lubbock, TX 79409, USA*
[b] *U.S. Geological Survey, 431 National Center, Reston, VA 20192, USA*
[c] *U.S. Geological Survey, 2730 N. Deer Run Rd, Carson City, NV 89701, USA*
[d] *U.S. Geological Survey, 1505 Ferguson Ln, Austin, TX 78754, USA*
[e] *U.S. Geological Survey, 5338 Montgomery Blvd. NE, Suite 400, Albuquerque, NM 87109, USA*
[f] *Dept. Environ. & Geog. Sci., University of Cape Town, Private Bag X3, Rondebosch 7701, South Africa*
[g] *Department of Earth and Atmospheric Sciences, University of Nebraska-Lincoln, 217 Bessey Hall, Lincoln, NE 68588-0340, USA*
[h] *Carl Sagan Center at the SETI Institute, 189 Bernardo Ave., Mountain View, CA 94043, USA*
[i] *NASA Ames Research Center, Moffett Field, CA 94035, USA*
[j] *Department of Civil Engineering, SSN College of Engineering, Kalavakkam 603110, India*
[k] *Department of Geological Sciences, University of Delaware Newark, DE 19716, USA*
[l] *CB&I Federal Services, Lawrenceville, NJ 08648, USA*
[m] *U.S. Geological Survey, Tucson, AZ, USA*
[n] *U.S. Geological Survey, Menlo Park, CA, USA*
[o] *Institute of Ecology & Biodiversity (IEB), Santiago, Chile*
[p] *Departamento de Ecología, Pontificia Universidad Católica de Chile, Santiago, Chile*
[q] *Key Laboratory of Metallogeny and Mineral Assessment, Institute of Mineral Resources, Chinese Academy of Geological Sciences, Beijing 100037, China*
[r] *USAFSAM/OEC, Wright-Patterson AFB, OH 45433, USA*

Received 2 June 2014; accepted in revised form 7 May 2015; available online 14 May 2015

Abstract

Natural perchlorate (ClO_4^-) is of increasing interest due to its wide-spread occurrence on Earth and Mars, yet little information exists on the relative abundance of ClO_4^- compared to other major anions, its stability, or long-term variations in production that may impact the observed distributions. Our objectives were to evaluate the occurrence and fate of ClO_4^- in groundwater and soils/caliche in arid and semi-arid environments (southwestern United States, southern Africa, United Arab Emirates, China, Antarctica, and Chile) and the relationship of ClO_4^- to the more well-studied atmospherically deposited anions NO_3^- and Cl^- as a means to understand the prevalent processes that affect the accumulation of these species over various time scales. ClO_4^- is globally distributed in soil and groundwater in arid and semi-arid regions on Earth at concentrations ranging from 10^{-1} to 10^6 μg/kg. Generally, the ClO_4^- concentration in these regions increases with aridity index,

* Corresponding author.
E-mail address: andrew.jackson@ttu.edu (W.A. Jackson).

http://dx.doi.org/10.1016/j.gca.2015.05.016

but also depends on the duration of arid conditions. In many arid and semi-arid areas, NO_3^- and ClO_4^- co-occur at molar ratios (NO_3^-/ClO_4^-) that vary between ~10^4 and 10^5. We hypothesize that atmospheric deposition ratios are largely preserved in hyper-arid areas that support little or no biological activity (e.g. plants or bacteria), but can be altered in areas with more active biological processes including N_2 fixation, N mineralization, nitrification, denitrification, and microbial ClO_4^- reduction, as indicated in part by NO_3^- isotope data. In contrast, much larger ranges of Cl^-/ClO_4^- and Cl^-/NO_3^- ratios indicate Cl^- varies independently from both ClO_4^- and NO_3^-. The general lack of correlation between Cl^- and ClO_4^- or NO_3^- implies that Cl^- is not a good indicator of co-deposition and should be used with care when interpreting oxyanion cycling in arid systems. The Atacama Desert appears to be unique compared to all other terrestrial locations having a NO_3^-/ClO_4^- molar ratio ~10^3. The relative enrichment in ClO_4^- compared to Cl^- or NO_3^- and unique isotopic composition of Atacama ClO_4^- may reflect either additional *in-situ* production mechanism(s) or higher relative atmospheric production rates in that specific region or in the geological past. Elevated concentrations of ClO_4^- reported on the surface of Mars, and its enrichment with respect to Cl^- and NO_3^-, could reveal important clues regarding the climatic, hydrologic, and potentially biologic evolution of that planet. Given the highly conserved ratio of NO_3^-/ClO_4^- in non-biologically active areas on Earth, it may be possible to use alterations of this ratio as a biomarker on Mars and for interpreting major anion cycles and processes on both Mars and Earth, particularly with respect to the less-conserved NO_3^- pool terrestrially.

1. INTRODUCTION

The oxyanion perchlorate (ClO_4^-) has received increasing attention due to its widespread occurrence on Earth and Mars, and yet its distribution and relation to other more understood atmospheric species are poorly defined. Terrestrial ClO_4^- is largely produced in the atmosphere and deposited in dry and wet deposition (Rajagopalan et al., 2009; Andraski et al., 2014). It is abiotically stable in most near-surface environments but can be irreversibly reduced biologically under anoxic conditions. In these respects ClO_4^- is similar to NO_3^-, although NO_3^- may be biologically reduced preferentially to ClO_4^- in mixed redox conditions. Major differences between the two species include a biological production mechanism for NO_3^- (nitrification) and the assimilation of NO_3^- by plants, from which N may be removed from the NO_3^- reservoir into stored organic matter or returned through subsequent nitrification. The terrestrial NO_3^- mass balance is complicated further by varying amounts of N_2 fixation, which may result in net changes to the free NO_3^- reservoirs in soils and groundwaters. Given these attributes, NO_3^- and ClO_4^- should co-occur in arid environments. In the driest and coldest locations, where biological activity is minimal, the ratio of NO_3^-/ClO_4^- should be similar to that of total atmospheric deposition; whereas in less arid environments, NO_3^-/ClO_4^- ratios could be higher or lower than the deposition ratio, depending on the relative importance of net biologic NO_3^- (or N) addition or removal. Further, the isotopic composition of NO_3^- in relation to the NO_3^-/ClO_4^- ratio should be consistent with the net effects of mixing of atmospheric and biogenic NO_3^-, commensurate with the degree of assimilation and reprocessing of the NO_3^- atmospheric fraction. Such a conceptual model can be used to evaluate environmental conditions under which atmospherically deposited species accumulate and the net effects of soil processes on these species.

Until recently, ClO_4^- was considered to be present in the environment largely from military and commercial sources, but its occurrence in pre-industrial soils and groundwater in the Atacama Desert (Ericksen, 1981), Antarctic Dry Valleys (Kounaves et al., 2010; Jackson et al., 2012), Mojave Desert and Southern High Plains (Jackson et al., 2010), Middle Rio Grande Basin (Plummer et al., 2006), as well as on the surface of Mars (Hecht et al., 2009; Glavin et al., 2013), all demonstrate that ClO_4^- forms naturally. Isotope data including $\Delta^{17}O$ and $^{36}Cl/Cl$ values of natural ClO_4^- indicate that it is produced largely in the stratosphere from oxidative reactions of chloro-oxyanions by O_3 oxidation and/or perhaps UV-mediated photo-oxidation (Bao and Gu, 2004; Sturchio et al., 2009; Jackson et al., 2010). ClO_4^- is deposited at the Earth's surface by wet and dry atmospheric deposition. Modern ClO_4^- wet deposition rates measured in North America averaged 64 mg/ha-year (Rajagopalan et al., 2009) and total deposition rates measured in the Amargosa Desert (southwestern Nevada) over a 6-year period averaged 343 mg/ha-year (Andraski et al., 2014). Accumulations of ClO_4^- (93–1050 g/ha) have been observed in deep unsaturated-zone salt bulges throughout the southwestern United States (U.S.) that accumulated during the late Quaternary, roughly over the last 100,000–10,000 years based on Cl^- deposition rates and inventories (Rao et al., 2007).

ClO_4^- is abiotically unreactive under typical terrestrial conditions but can be microbially (Archea and Bacteria) reduced under anoxic conditions as an electron acceptor (Coates and Achenbach, 2004; Liebensteiner et al., 2013). Reduction of ClO_4^- can be coupled to oxidation of various electron donors including organic matter, sulfide, and H_2. In electron donor-limited environments, the presence of NO_3^- at greater concentrations has been shown to inhibit ClO_4^- reduction (Tan et al., 2004a; Farhan and Hatzinger, 2009). The capacity for ClO_4^- reduction appears to be common and has been demonstrated in a number of environments including Antarctic Dry Valley lakes (Jackson et al., 2012). Plants accumulate ClO_4^- primarily in transpiring tissue (e.g. leaves) (Jackson et al., 2005; Voogt and Jackson, 2010), and do not generally appear to transform it substantially (Tan et al., 2006; Seyfferth et al., 2008), although this may occur in some cases (Van Aken and

Schnoor, 2002). Bioaccumulated ClO_4^- can be returned to the environment by senescence and leaching of plant tissue (Tan et al., 2004b, 2006; Andraski et al., 2014).

The largest and best known occurrence of terrestrial ClO_4^- is in the NO_3^- deposits of the Atacama Desert (Erickson, 1981; Pérez-Fodich et al., 2014). Elevated ClO_4^- concentrations also have been reported in the clay hills near Death Valley (Jackson et al., 2010; Lybrand et al., 2013), subsurface salt accumulations in the southwestern U.S. (Rao et al., 2007), surface soils of the Dry Valleys of Antarctica (Kounaves et al., 2010), and surface soils in northeastern China (Ye et al., 2013) and the Amargosa Desert (Andraski et al., 2014). These occurrences have been interpreted to be of natural origin based on the distribution and age of the accumulations and /or the stable isotopic composition of the ClO_4^- and coexisting NO_3^-. ClO_4^- has also been reported in groundwater and surface water in many areas including China, India, South Korea, Antarctica, and the U.S. (Plummer et al., 2006; Rajagopalan et al., 2006; Quinones et al., 2007; Parker et al., 2008; Kannan et al., 2009; Ye et al., 2013). Some of these occurrences could be related to human activities including release of electrochemically produced ClO_4^- and distribution of NO_3^- fertilizers containing ClO_4^- from the Atacama Desert. Other occurrences are interpreted to be indigenous based on location, groundwater age, and/or stable isotopic composition (Plummer et al., 2006; Rajagopalan et al., 2006; Jackson et al., 2010, 2012; Kounaves et al., 2010).

Here we present new data for natural ClO_4^- occurrences in selected globally distributed settings and an overview of the factors controlling ClO_4^- accumulation in the environment. We measured indigenous ClO_4^- concentrations in soil/caliche and groundwater samples from a variety of arid and semi-arid locations in Antarctica, Chile, China, southern Africa, United Arab Emirates (UAE), and the U.S. We also investigated the relationship between ClO_4^- and co-occurring Cl^- and NO_3^- as well as the sources and sinks of NO_3^- based on isotope data ($\delta^{15}N$, $\delta^{18}O$, and $\Delta^{17}O$). Our objectives were to evaluate the occurrence and fate of ClO_4^- in arid environments and the relationship of ClO_4^- to the better studied atmospherically deposited species NO_3^- and Cl^- as a means to understand the prevalent processes that affect the accumulation of these species over various time scales. We developed a conceptual model of ClO_4^- occurrence in relation to NO_3^- that incorporates the overall impact of biological processes to the co-occurrence of these important oxyanions. Our results firmly establish the widespread global occurrence of ClO_4^-, provide insights about environmental conditions controlling its distribution, and appear to indicate a new approach for evaluating arid-region biogeochemistry with particular relevance to NO_3^- processing and Cl^- cycling. Our results also may contribute to understanding the prevalence of ClO_4^- on Mars and its implications to the co-occurrence of NO_3^- and possible extraterrestrial biologic impacts on these species (Stern et al., 2015).

2. MATERIALS AND METHODS

Soil, unsaturated subsoil, caliche-type salt deposits, and groundwater samples were collected for this study or obtained from archived samples of previous studies from sites in the U.S., Southern Africa (Namibia, South Africa, and Botswana), UAE, China, Chile, and Antarctica (Fig. 1). Sample sites are described below and summarized in Tables 1 and 2. All samples were analyzed for Cl^-, NO_3^-, and ClO_4^- concentrations and a subset was evaluated for NO_3^- stable isotopic composition as described below.

2.1. Site and sample descriptions

2.1.1. United States

2.1.1.1. Mojave desert-soil. Near surface soil samples (composites) from areas of desert pavement and subsoil samples from discrete depths were collected in the northern Mojave Desert near the U.S. Geological Survey (USGS) Amargosa Desert Research Site (Fig. 1) (Andraski et al., 2014). The Amargosa Desert, in the Basin and Range Province, is bounded by block-faulted mountains composed of Paleozoic metamorphic rocks and Tertiary volcanic rocks. Moderate to steep sloping alluvial fans near the foot of the mountains and the valley floor have sparse, mixed vegetation dominated by creosote bush (*Larrea tridentata*). Discrete-depth soil and/or salt-rich caliche were also collected from three sites (Bully Hill, Confidence Hills, Saratoga Hills) in the southern Death Valley region. The Death Valley sites are unvegetated clay hills formed from steeply tilted sedimentary beds and were previously studied for their unusual surface concentrations of NO_3^- and more

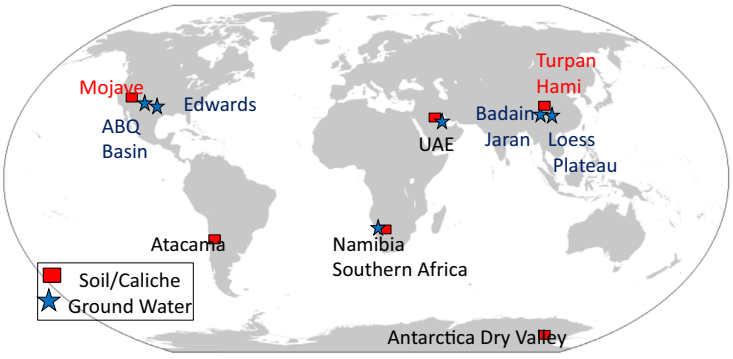

Fig. 1. Map of sample locations.

Table 1
Locations, sample types, summary statistics for ClO_4^-, NO_3^-, and Cl^- in groundwater and deposition sample sets. Molar ratios are averages of log-transformed ratios. *r* and *P* values are for linear regressions (see Fig. 2).

Location	Site	Sample type	Molar ratio			NO_3 and ClO_4		Cl and ClO_4		Cl and NO_3	
			NO_3/ClO_4	Cl/ClO_4	Cl/NO_3	*r*	*P*	*r*	*P*	*r*	*P*
All GW			24,000	240,000	15	0.98	<0.001	0.87	<0.001	0.92	<0.001
United States	Edwards Aquifer	Public supply/Monitoring	22,000	96,000	4.3	0.22	0.04	0.27	0.01	−0.07	0.46
	Albuquerque Basin	Supply/Monitoring	22,000	300,000	14	0.82	<0.001	0.22	0.13	0.05	0.69
China	Loess Plateau	Springs	11,000	47,000	5.4	0.95	<0.001	0.15	0.69	0.35	0.33
	Badain Jaran	Shallow wells/Springs	61,000	1,000,000	17	0.57	0.01	0.37	0.11	0.20	0.4
Namibia		Springs/well	29,000	2,300,000	81	0.91	<0.001	0.89	0.001	0.96	<0.001
UAE		Supply and monitoring wells	22,000	550,000	25	0.98	<0.001	0.95	<0.001	0.94	<0.001
Deposition											
United States[a]	18 sites across U.S.	Wet deposition	100,000	35,000	0.34	0.7	<0.001	0.52	<0.01	0.5[c]	0.01
United States[b]	Mojave	Total deposition	22,000	6,600	0.33	0.89	<0.01	0.84	<0.01	0.89	<0.01

[a] Rajagopalan et al. (2009).
[b] Andraski et al. (2014).
[c] Excludes coastal sites from analysis.

recently for co-occurring ClO_4^- (Ericksen et al., 1988; Böhlke et al., 1997; Michalski et al., 2004; Jackson et al., 2010; Lybrand et al., 2013). We also obtained archived (filtered and aerated) soil leachates from previous studies of indigenous NO_3^- in the Rainbow Hills and Fort Irwin Basin in the western Mojave Desert (Böhlke et al., 1997; Densmore and Böhlke, 2000). The Mojave Desert sites receive variable rainfall but generally less than 10 cm/year.

2.1.1.2. Edwards aquifer-groundwater. Groundwater samples were collected from the San Antonio segment of the fractured karstic Edwards aquifer in Texas, (U.S.) as part of the USGS National Water-Quality Assessment Program (Fig. 1) (Musgrove et al., 2010). Groundwater samples were collected in accordance with procedures described in Koterba and others (1995) and in the USGS National Field Manual. Water samples were collected from public-supply wells in 2004–05 and from a combination of public, domestic, stock, and commercial supply and monitoring wells in 2006. Public-supply well depths ranged from about 65 to 716 m; domestic, commercial, and stock well depths ranged from 24 to 152 m; and monitoring-well depths ranged from 55 to 98 m. The climate is subtropical sub-humid. Mean annual precipitation decreases across the region from 86 cm/year in the east to 56 cm/year in the west (Bomar, 1994). Groundwater from the sampled portion of the Edwards aquifer was recharged predominantly within approximately the past 50 years and mixed extensively in the subsurface, and the whole aquifer is susceptible to anthropogenic impacts (Musgrove et al., 2010).

2.1.1.3. Albuquerque basin-groundwater. In the Albuquerque (ABQ) Basin, New Mexico, U.S., groundwater samples were collected from public-supply wells in 2005 and from public-supply and monitoring wells in 2007–2009 (Fig. 1). Public-supply well depths ranged from about 65 to 630 m and monitoring-well depths ranged from about 80 to 360 m. Groundwater samples were collected in accordance with USGS procedures cited above. The climate is semiarid, with potential evaporation substantially exceeding mean annual precipitation (22.1 cm/year at Albuquerque during 1914–2010). The ABQ alluvial basin consists largely of unconsolidated to moderately consolidated deposits of sand, gravel, silt, and clay. The age of most groundwater in the basin is on the order of thousands of years (Plummer et al., 2004; Bexfield et al., 2011).

2.1.2. Southern Africa-soil and groundwater

Soil samples collected in southern Africa were primarily from the hyper-arid Central Namib gravel plains (Fig. 1). Samples represent composites (0–30 cm depth) from locations in an area covering ~150 km north to south and up to 85 km west to east from the coast. Rainfall for all sites is below 10 cm/year and may be as low as 0 cm/year. The eastern-most soil samples were from a calcrete-rich substrate and include the Zebra Pan, a small recharge playa. The central and western soil samples were from gypcrete-rich pediment characterized by lag gravel, fog precipitation, and lichen growth, and they include a sample from Eisfeld, a saline discharge spring and playa. Samples

Table 2
Locations, sample types, summary statistics for ClO_4^-, NO_3^-, and Cl^- in soil/caliche sample sets. Molar ratios are averages of log-transformed ratios. *r* and *P* values are for linear regressions (see Fig. 5) .

Location	Site	Sample type	Sample depth range (m)	Molar ratio			NO_3 and ClO_4		Cl and ClO_4		Cl and NO_3	
				$NO_3/ClO4$	Cl/ClO_4	Cl/NO_3	*r*	*P*	*r*	*P*	*r*	*P*
United States-Mojave	Total			85,000	580,000	6.7	0.66	<0.001	0.18	0.06	0.42	<0.001
	Saratoga Hills	Profile	0–0.4	114,000	7,400,000	65	0.14	0.84	−0.56	0.33	−0.08	0.9
	Bully Hill	Profile	0–0.9	240,000	300,000	1.3	0.87	0.06	0.79	0.06	0.98	0.002
	Confidence Hills	Profile	0–1.0	115,000	7,400,000	65	0.89	0.02	0.23	0.66	0.47	0.35
	Confidence Hills	Profile	0–0.3	41,000	530,000	13	0.98	0.002	0.08	0.89	0.04	0.95
	Confidence Hills	Profile	0–0.7	25,000	6,300,000	174	0.99	<0.001	0.72	0.17	0.97	0.03
	Confidence Hills	Profile	0–0.3	110,000	141,000	1.3	0.28	0.72	0.24	0.76	0.77	0.23
	Confidence Hills	Profile	0–0.4	91,000	480,000	5.2	0.30	0.62	−0.31	0.61	0.80	0.1
	Desert Pavement	Composite	0–0.3	86,000	100,000	1.2	0.90	0.01	0.81	0.05	0.96	0.002
	Desert Pavement	Profile	0–0.6	72,000	77,000	1.3	0.99	<0.001	0.99	<0.001	0.99	<0.001
	Subsurface Salt Bulge	Profile	0–16	40,000	190,000	4.6	0.92	<0.001	0.64	0.001	0.75	<0.001
	Rainbow Hills	Grab	0–4	230,000	216,000	1.0	0.99	0.002	0.99	0.001	0.99	0.01
	Fort Irwin	Profile		216,000	709,000	3.53	0.61	0.2	0.04	0.93	0.59	0.22
Southern Africa	Total			120,000	2,700,000	22	0.79	<0.001	−0.01	0.96	<0.08	0.67
	Namibia	Composite	0–0.3	96,000	730,000	7.3	0.81	<0.001	0.07	0.77	−0.05	0.82
	South Africa	Composite	0–0.3	150,000	650,000	4.4	0.99	0.06	0.93	0.25	0.96	0.18
	Botswana	Composite	0–0.3	125,000	41,000,000	330	0.96	<0.001	0.52	0.23	0.53	0.23
UAE				21,000	870,000	42	0.99	<0.001	0.54	0.11	0.25	0.40
	Soils	Composite	0–0.3	14,000	19,000	1.1	0.87	0.05	0.03	0.96	0.41	0.36
	Sabkha	Composite	0–1	28,000	1,700,000	82	0.99	<0.001	0.15	0.81	−0.12	0.8
Atacama	Total			1400	1500	1.1	0.63	<0.001	0.26	0.006	0.66	<0.001
	AT6	Profile	0–1.5	2200	4700	2.3	0.74	0.002	0.59	0.02	0.48	0.08
	AT8	Profile	0–2.0	570	1500	2.7	0.65	0.002	0.53	0.02	0.52	0.02
	AT9	Profile	0–1.9	730	1100	1.5	0.91	<0.001	0.61	0.08	0.38	0.31
	AT16	Profile	0–0.7	13,000	1300	0.1	0.98	<0.001	0.48	0.33	−0.50	0.31
	AT18	Profile	0–3.0	1600	1200	0.7	0.77	<0.001	0.74	0.002	0.93	<0.001
	Mine	Profile	0–3.0	550	615	1.1	0.32	0.22	0.86	<0.001	0.93	<0.001
	Transect	Composite	0–0.3	1000	2200	2.1	0.93	<0.001	−0.1	0.69	0.2	0.44
China	Turpan-Hami	Grab	<2	12,000	190,000	17	0.61	0.05	−0.29	0.39	−0.56	0.07
Antarctica McMurdo Dry Valley-University	Total		<0.7	14,000	7200	0.35	0.78	<0.001	0.81	<0.001	0.75	<0.001
	1	Profile	0–0.36	11,000	4,600	0.46	0.83	<0.001	0.72	0.002	0.66	0.006
	2	Profile	0–0.40	20,000	6,700	0.34	0.99	<0.001	0.99	<0.001	0.99	<0.001
	3	Profile	0–0.56	7,900	5,000	0.66	0.98	<0.001	0.99	<0.001	0.97	<0.001
	4	Profile	0–0.66	11,000	8,100	0.87	0.86	<0.001	0.98	<0.001	0.79	0.004
	5	Profile	0–0.66	19,000	10,000	0.68	0.75	0.03	0.97	<0.001	0.77	0.03
	7	Profile	0–0.16	13,000	8,100	0.64	0.98	0.004	0.82	0.09	0.76	0.13

from Goanikontes were taken at a 20 m high escarpment and include top (A), middle (B) and bottom (C) slopes. A small set of Namibia water samples (springs, potholes, and one groundwater sample) were also obtained from the same region. Additional soil samples were obtained from saline playa surfaces in South Africa (Kalahari Desert; Haskenpan, Koppieskraal and Nolokei) and in Botswana (Makgadikgadi).

2.1.3. United Arab Emirates (UAE)—soil and groundwater

Soil and groundwater samples were collected from a number of sites in the UAE (Emirate of Abu Dhabi). Soil-surface (0–30 cm) composite samples were from undisturbed areas and discrete-depth samples were from two hand-dug pits in the coastal Sabkha. Groundwater samples were collected from production wells ($n = 12$), monitoring wells ($n = 3$), and shallow hand-dug pits ($n = 2$). Groundwater samples were collected from wells near agricultural areas of Mohayer, Ghayathi, and Liwa. Soil samples were collected from the coastal Sabkha, Matti, and Gayathi regions. The climate is subtropical arid. Rainfall varies across the UAE with reported modern (1966–1998) rainfall ranging from 7 to 13 cm/year, with a high potential evaporation rate of about 2–3 m/year (Sherif et al., 2014).

2.1.4. Atacama desert-soil/caliche

Surface-soil samples (0–30 cm composites) were collected along an elevational transect east of Antofagasta, Chile, extending from the Baquedano nitrate mining district in the 'absolute desert' (~1300 m) (i.e., a plant-free

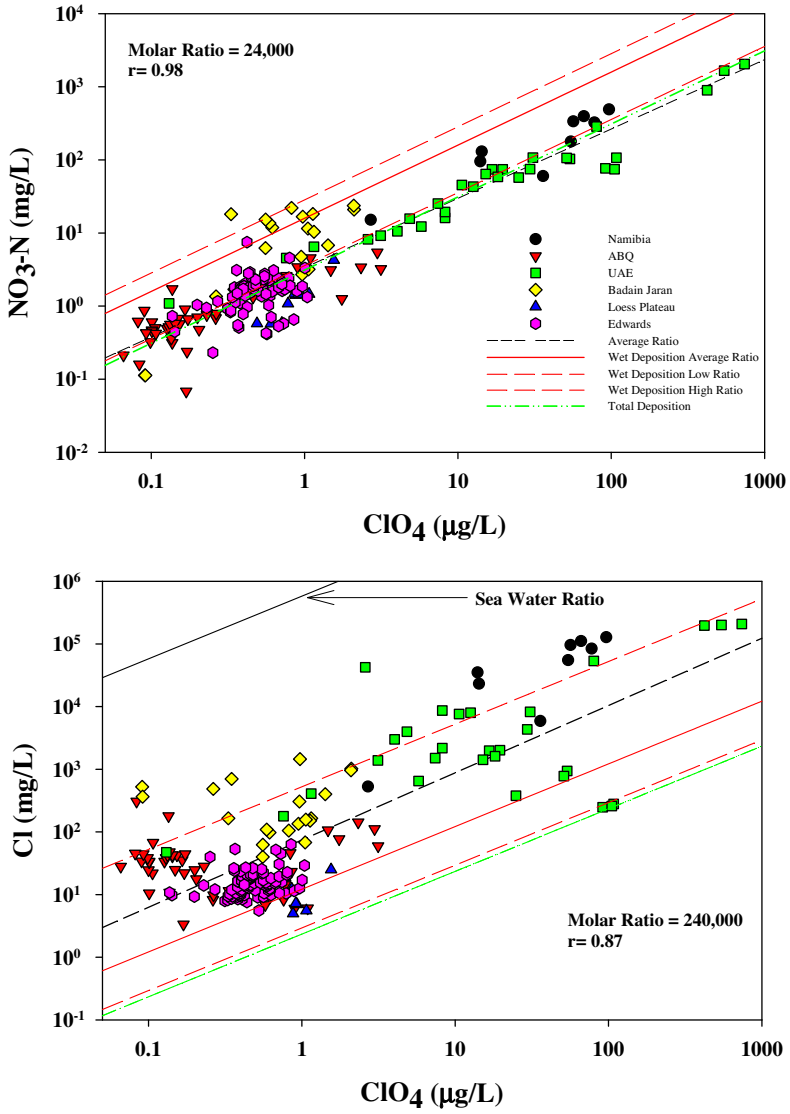

Fig. 2. Relations among ClO_4^-, NO_3^-, and Cl^- concentrations in groundwater. Ratios for all groundwater samples are shown by solid black lines. Average ratios in U.S. wet deposition are shown as solid red lines, and minimum and maximum average site ratios are shown as dashed lines. Ratios for wet deposition include 18 sites located across the conterminous U.S., as well as Alaska, and Puerto Rico for weekly samples over a three year period Rajagopalan et al. (2009). The total deposition ratio (green line) represents the 6 year average of quarterly samples Andraski et al. (2014).

landscape) to the tussock steppe grasslands of the Western Andes Cordillera (4200 m) (Fig. 1). Discrete-depth samples were collected from existing or fresh hand excavated pits within 25–75 km of the coast along a 450 km north–south transect. Additional discrete-depth samples were collected from open faces within an active nitrate mine. Atacama NO_3^- mineral deposits are considered to have accumulated over a period of the order of 10^6–10^7 years (Pérez-Fodich et al., 2014). The Atacama Desert is a hyper-arid cold desert with estimates of average annual rainfall less than 0.01 cm/year with large stretches of absolute desert.

2.1.5. China-soil and groundwater

2.1.5.1. Turpan-Hami-caliche. Caliche-type salt-rich samples were obtained from three sub-basins (Kumutage, Wuzongbulake, and Xiacaohu) in the Turpan-Hami Depressions, an area of fault-bounded troughs that descend to below sea level in northwestern China (Fig. 1). Samples from Kumutage are from a vertical profile (0–2 m depth), whereas samples from the other basins are from unknown depths. These sites are associated with recently described massive NO_3^- deposits (Qin et al., 2012). The NO_3^- from this region has a wide range of stable isotopic composition, ranging from predominantly un-cycled atmospheric to predominantly biogenic NO_3^-. The deposits are estimated to be <260 k years old (Qin et al., 2012). Climate in the region is hyper-arid, with precipitation <1.5 cm/year.

2.1.5.2. Loess Plateau-groundwater. Archived (filtered and refrigerated) water samples were obtained from a previous study evaluating groundwater recharge in the central Loess Plateau in Shaanxi Province, China (Gates et al., 2011). Samples were originally collected in 2008. The sampled area has an elevation of ~1000–2000 m above sea

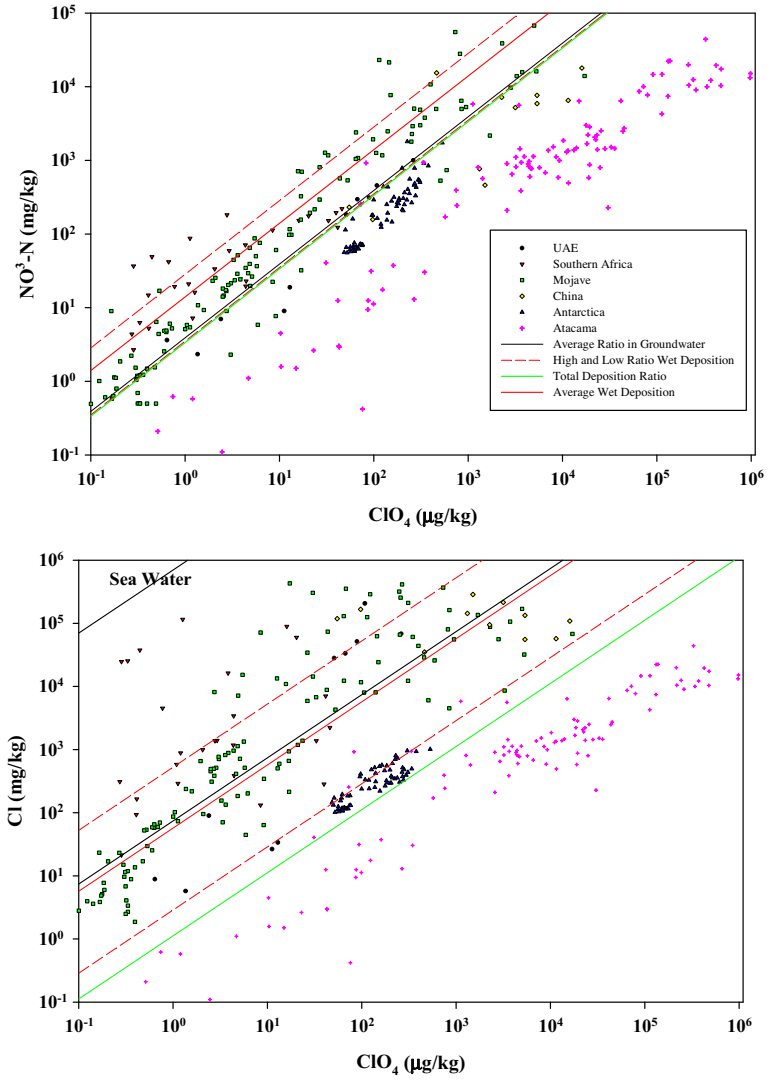

Fig. 3. Relations between concentrations of ClO_4^- and NO_3^- and Cl^- for all soils and caliches. Average ratio in wet deposition is shown as solid red lines, and average minimum and maximum ratios for all sites are shown as dashed lines. Ratios for wet deposition include 18 sites located across the conterminous U.S., Alaska, and Puerto Rico for weekly samples over a three year period Rajagopalan et al. (2009). The total deposition ratio (green line) represents the 6 year average of quarterly samples Andraski et al. (2014).

level. Approximately 20% of the catchment land area is cultivated (primarily dryland wheat farming). Mean annual rainfall is ~50 cm/year. Groundwater is >100 m deep in upland areas and discharges into incised valleys. The samples were collected from springs over a range of elevations (1036–1231 m).

2.1.5.3. Badain Jaran-groundwater. Archived (filtered and refrigerated) groundwater samples were obtained from a previous study of shallow wells and springs located near the margin between the Badain Jaran dune field and Yabulai Mountains, Gurinai Grass Land, and Xugue Lake area (Fig. 1) (Gates et al., 2008a,b). The area is sparsely settled and contains only limited vegetative cover on unconsolidated sand dunes interspersed with groundwater-fed lakes of varying salinity. The dune area is underlain by a shallow surficial aquifer that is locally confined in some areas. Previous studies indicate groundwater recharge occurs largely at higher elevations near the margins of the basin. The area is considered a cold continental desert with average (1956–1999) precipitation of 8.4 cm/year (Gates et al., 2008a).

2.1.6. Antarctica-soil

Discrete depth samples were collected from shallow hand dug pits in University Valley (1600 m), which is a perched valley above Beacon Valley in the Quartermain range of the McMurdo Dry Valley (MDV) region of Antarctica (Fig. 1). University Valley and nearby valleys contain elevated concentrations of NO_3^- primarily of atmospheric origin (Michalski et al., 2005) as well as elevated concentrations of ClO_4^- (Kounaves et al., 2010). University Valley is located in a hyper-arid region of the MDV and receives a current water equivalent precipitation of less than 5 cm/year.

2.2. Soil extraction methods

Soluble salts from soil samples were extracted by mixing the soil with Milli-Q water at a 5:1 ratio (mass of water: mass of soil) and shaking for 24 h. The samples were centrifuged for 10 min, after which the supernatant was decanted and filtered (0.2 μm). All extraction sets were accompanied by an extraction duplicate and extraction sample spike (soil + known amount of ClO_4^- spike), extraction blank (DDI water only), and extraction spike (known amount of ClO_4^- spike). Moisture contents of samples were determined by drying at 105 °C for 24 h. Sub-samples of some extracts were preserved at pH~11 for analysis of NO_3^- stable isotopic composition.

2.3. Analytical methods

Analysis of soil extracts and groundwater for ClO_4^-, NO_3^-, Cl^-, and NO_3^- stable isotopic composition has been described previously (Jackson et al., 2010). Briefly, ClO_4^- was quantified using an ion chromatograph-tandem mass spectrometry technique (IC–MS/MS) that consisted of a GP50 pump, CD25 conductivity detector, AS40 automated sampler and Dionex IonPac AS16 (250 × 2 mm) analytical column. The IC system was coupled with an Applied Biosystems – MDS SCIEX API 2000™ triple quadrupole mass spectrometer equipped with a Turbo-IonSpray™ source. A 45 mM hydroxide (NaOH) eluent at 0.3 ml min^{-1} was followed by 90% acetonitrile (0.3 ml min^{-1}) as a post-column solvent. To overcome matrix effects, all samples were spiked with an oxygen-isotope (^{18}O) labeled ClO_4^- internal standard. A 25 μL loop was used for sample loading with a 0.0005 μM level of quantification. Chloride and NO_3^- were analyzed following EPA Method 300.0 using a Dionex LC20, an IonPac AS14A column (4 × 250 mm), 8 mM Na_2CO_3/1 mM $NaHCO_3$ eluent, and an Anion Atlas electrolytic suppressor. The limit of detection (LOD) of Cl^- and NO_3^- were 1.4 μM and 3.5 μM, respectively. Individual sample quantification limits were based on the final dilution of the sample extract.

$\delta^{15}N$ and $\delta^{18}O$ in NO_3^- were measured by continuous-flow isotope-ratio mass spectrometry on N_2O produced from NO_3^- by bacterial reduction (Sigman et al., 2001; Casciotti et al., 2002; Coplen et al., 2004). The data were calibrated by analyzing NO_3^- isotopic reference materials as samples and normalizing to $\delta^{15}N$ and $\delta^{18}O$ reference values (Böhlke et al., 2003; Jackson et al., 2010). For samples with elevated $\Delta^{17}O$ of NO_3^-, $\delta^{15}N$ values determined by the bacterial N_2O method using conventional normalization equations may be slightly higher than true values (Sigman et al., 2001; Böhlke et al., 2003; Coplen et al., 2004). $\delta^{15}N$ values reported here were not adjusted for this effect because $\Delta^{17}O$ values were not measured in all samples. True $\delta^{15}N$ values could be lower than reported values by varying amounts ranging from 0‰ for biogenic NO_3^- with $\delta^{18}O$ and $\Delta^{17}O$ near 0‰ to around 1.6‰ for atmospheric NO_3^- from Antarctica with the highest $\delta^{18}O$ and $\Delta^{17}O$ values.

For selected samples, the $\Delta^{17}O$ value of NO_3^- was measured by dual-inlet isotope-ratio analysis of O_2 produced by off-line partial decomposition of $AgNO_3$ (modified from Michalski et al., 2002). NO_3^- was isolated from mixed salt solutions by trapping on large-volume AG1X8 ion-exchange resin columns, followed by gradual elution with 0.5 M KCl to separate anions (Hannon et al., 2008). The KCl^-–KNO_3 eluent was passed through AG-MP50 cation-exchange resin columns in the Ag form to remove Cl and exchange K for Ag, then freeze dried to produce $AgNO_3$ salt. The $AgNO_3$ was heated under vacuum at 520 °C while connected to a 5A° mol-sieve trap cooled with liquid N_2 to collect O_2, which was then isolated and transferred to the mass spectrometer and analyzed against tank O_2. Measured $\Delta^{17}O$ values of NO_3^- isotopic reference materials RSIL-N11 and USGS35 prepared as $AgNO_3$ were indistinguishable from reported values of −0.2 and +21.1‰, respectively, as defined in Böhlke et al. (2003).

2.4. Data analysis

Average molar ratios were calculated by averaging log-transformed individual sample ratios and then back transforming to standard notation. This was done to reduce the impact of individual samples with order of magnitude differences in ratios. Regression analysis was performed

on data as presented in figures and significance was designated as $P < 0.05$.

3. RESULTS AND DISCUSSION

Results are summarized for all samples in Figs. 2 and 3 and Tables 1 and 2 to highlight major global patterns and processes affecting the distribution of ClO_4^- and NO_3^-. Results for individual sites and sample types are then presented in more detail in Figs. 4 and 5 to facilitate discussion of local patterns, controls, and exceptions to the global patterns.

3.1. Global patterns of ClO_4^- concentrations, NO_3^- concentrations, and NO_3^- isotopes

Combined data from this study indicate the global occurrence of ClO_4^- and positive correlation between NO_3^- and ClO_4^- concentrations in oxic groundwaters (Fig. 2, Table 1), and in soils and caliches (Fig. 3, Table 2), in arid and semi-arid environments. Previous work has largely attributed the source of indigenous natural ClO_4^- to atmospheric production and subsequent deposition (Rajagopalan et al., 2009; Jackson et al., 2010). Excluding the Atacama site, our results are generally consistent with this assertion based on similarities between site NO_3^-/ClO_4^- ratios and those previously reported. Atmospheric deposition data include wet deposition at 18 sites located across the conterminous U.S., Alaska, and Puerto Rico using weekly samples collected over 3 years (Rajagopalan et al., 2009) and total atmospheric deposition (wet plus dry including dust) collected over a 6 year period at the Amargosa Desert Research Site, Nevada (Andraski et al., 2014). The average molar ratios of NO_3^-/ClO_4^- in wet deposition ranged over ~one order of magnitude, while Cl^-/ClO_4^- ratios varied over 2 orders of magnitude and were significantly related to distance from a coast. NO_3^-/ClO_4^- and Cl^-/ClO_4^- molar ratios in total deposition were lower than in wet deposition and the NO_3^- was largely unaltered atmospheric, based on stable isotope ratios (Figs. 2, 3 and 6; Table 1).

In contrast to the relatively good correlation between NO_3^- and ClO_4^- at most sites, concentrations of Cl^- appear to be relatively poorly correlated with either NO_3^- or ClO_4^- for most sites (Figs. 4 and 5). Most samples had relatively high Cl^-/NO_3^- and Cl^-/ClO_4^- ratios compared to those of modern precipitation and total deposition in North America (Fig. 7). Local high deposition fluxes of marine (seasalt) Cl^- could account for some, but not all of these differences. Additional sources of Cl^- unrelated to the Cl^- deposited with ClO_4^- and NO_3^- could include local Cl^- atmospheric inputs remobilized from salt flats, upwelling of saline groundwater, and run-on of Cl^- laden water. Alternatively, high Cl^-/NO_3^- and Cl^-/ClO_4^- ratios could indicate simultaneous net loss of NO_3^- and ClO_4^- as a result of microbial reduction where moisture and organic matter were present (Nozawa-Inoue et al., 2005). This could have occurred during episodic events, defined as locally reducing conditions during individual precipitation wetting events that led to the depletion of oxyanions during the accumulation period of the current oxyanions. Cl^- remaining after such episodic reduction is hereafter referred to as "episodic

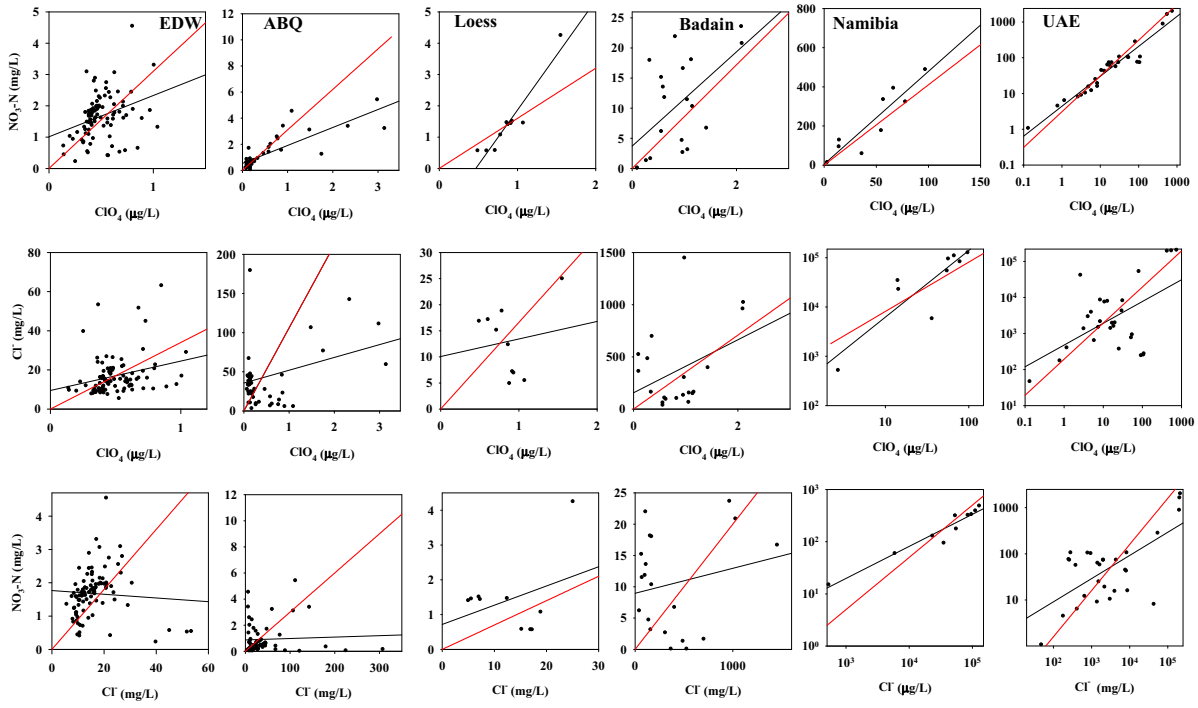

Fig. 4. Relations among ClO_4^-, NO_3^-, and Cl^- in groundwater from arid and semi-arid locations. Solid black lines represent linear regressions of concentration data; red lines represent averages of log-transformed ratios. Correlation coefficients and P values are listed in Table 1. (For interpretation of the references to color in this figure legend, the reader is referred to the web version of this article.)

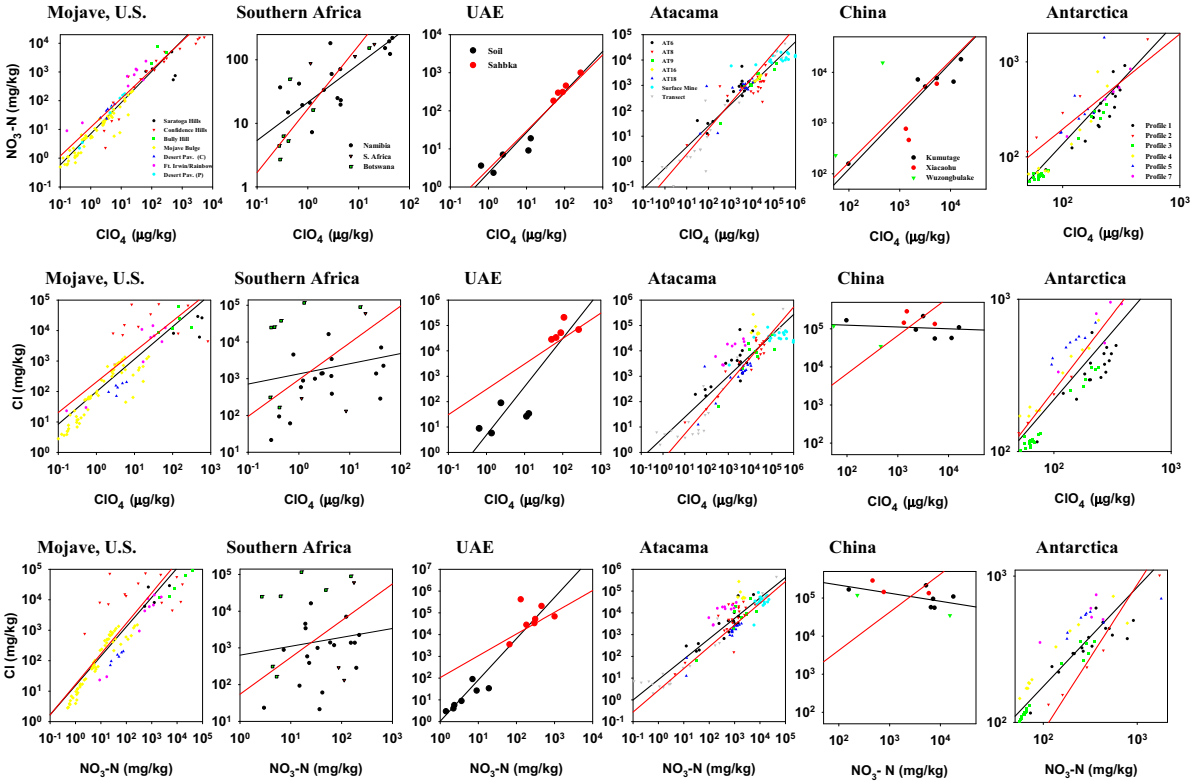

Fig. 5. Relations among ClO_4^-, NO_3^-, and Cl^- concentrations in soils and caliches from arid and semi-arid locations. Solid black lines represent linear regressions of concentration data; red lines represent averages of log – transformed ratios. Correlation coefficients and *P* values are listed in Table 2. (For interpretation of the references to color in this figure legend, the reader is referred to the web version of this article.)

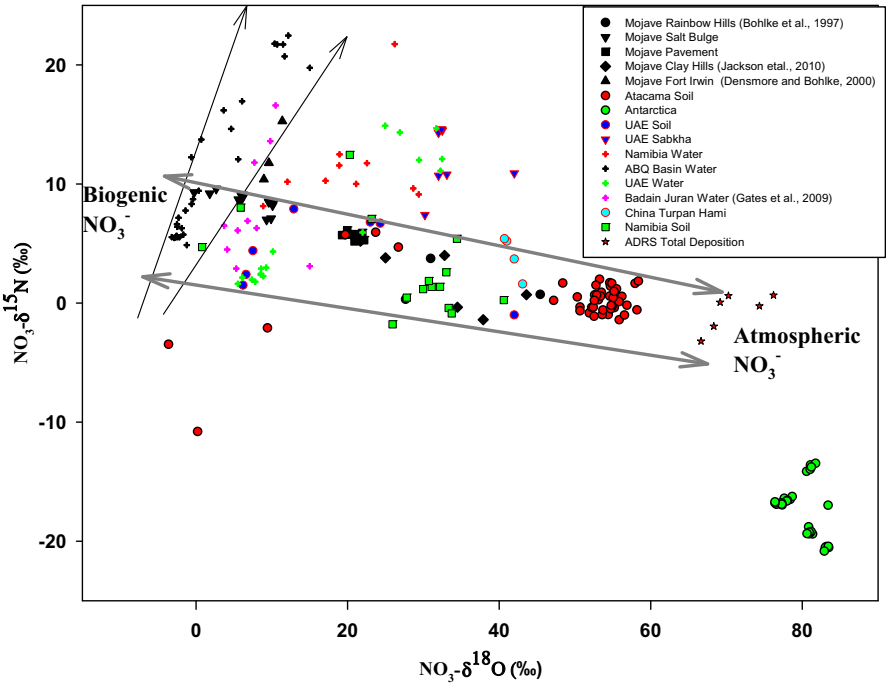

Fig. 6. Relation between $\delta^{15}N$ and $\delta^{18}O$ of NO_3^- in groundwater and leachate from soil and caliche samples. Black arrows represent the range of slopes reported previously for isotopic fractionation due to denitrification and grey arrows represent general trends in mixing ratios of atmospheric and biogenic NO_3^-.

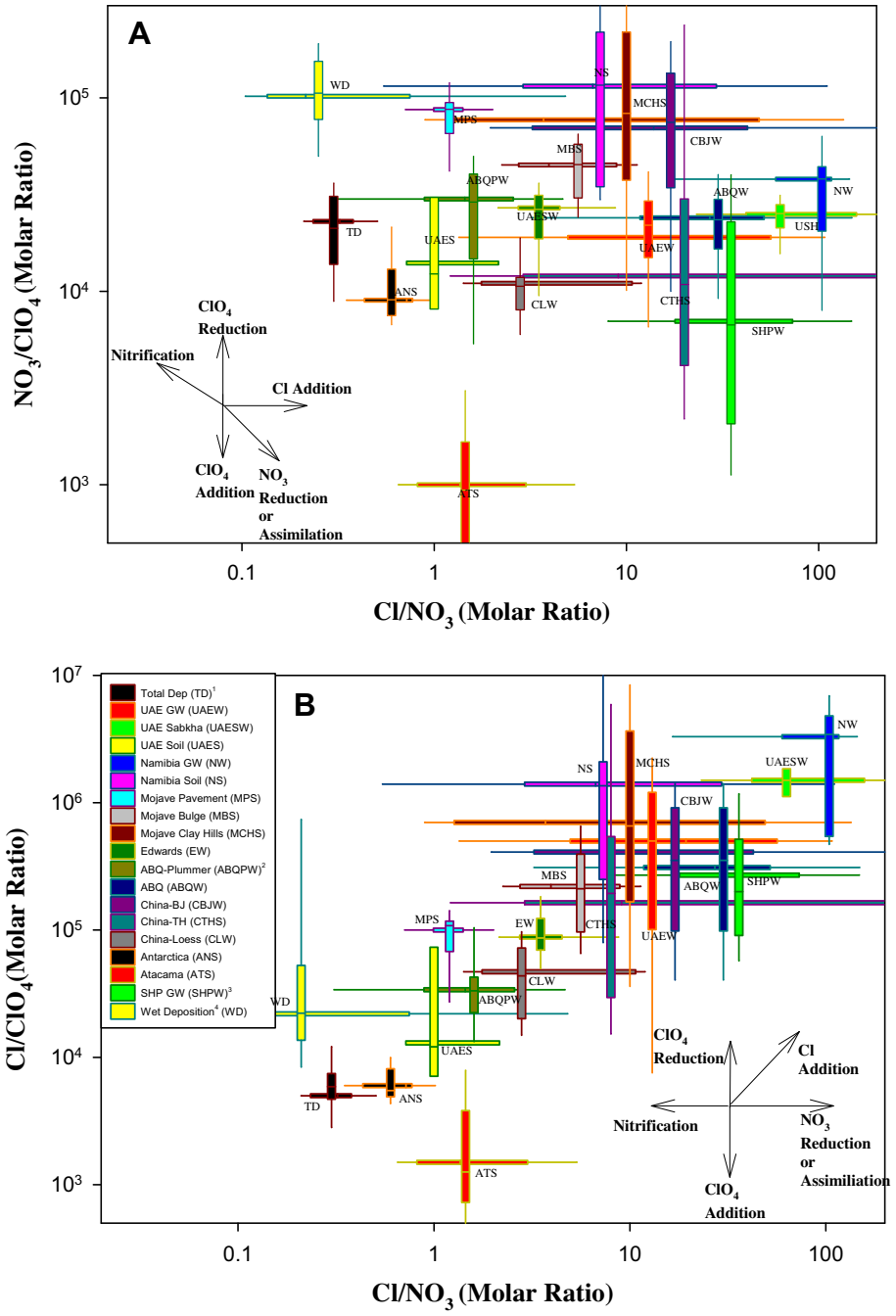

Fig. 7. Variation of (A) NO_3^-/ClO_4^- or (B) Cl^-/ClO_4^- ratios with respect to Cl/NO_3 ratios in soils and groundwaters from arid and semi-arid locations as well as wet and dry deposition in North America. Box plots represent the 25th and 75th percentile values and extended lines from boxes represent the 90th and 10th percentiles. Arrows indicate hypothetical qualitative trajectories that could be caused by various processes. ([1]Andraski et al., 2014; [2]Plummer et al., 2006; [3]Rajagopalan et al., 2006; [4]Rajagopalan et al., 2009).

Cl^-". Alternatively, oxyanions could have been depleted relative to Cl^- during prolonged periods of wetter climate in the past prior to the accumulation period of the observed oxyanions. For this case, we hereafter refer to atmospheric Cl^- not associated with the current NO_3^- and ClO_4^- as "non-co-deposited Cl^-".

Isotope data indicate sources of NO_3^- from these sites varied from essentially 100% unaltered atmospheric to 100% biogenic, where biogenic NO_3^- could be derived from various N sources including recycled atmospheric NO_3^- (Fig. 6). Collectively, isotopic analyses of NO_3^- are consistent with two major factors affecting $\delta^{15}N$ and $\delta^{18}O$ of NO_3^-: (1) variation in the relative proportions of atmospheric NO_3^- (low $\delta^{15}N$, high $\delta^{18}O$) and biogenic NO_3^- (high $\delta^{15}N$, low $\delta^{18}O$), yielding an overall negative correlation between $\delta^{15}N$ and $\delta^{18}O$, and (2) variation in the isotope

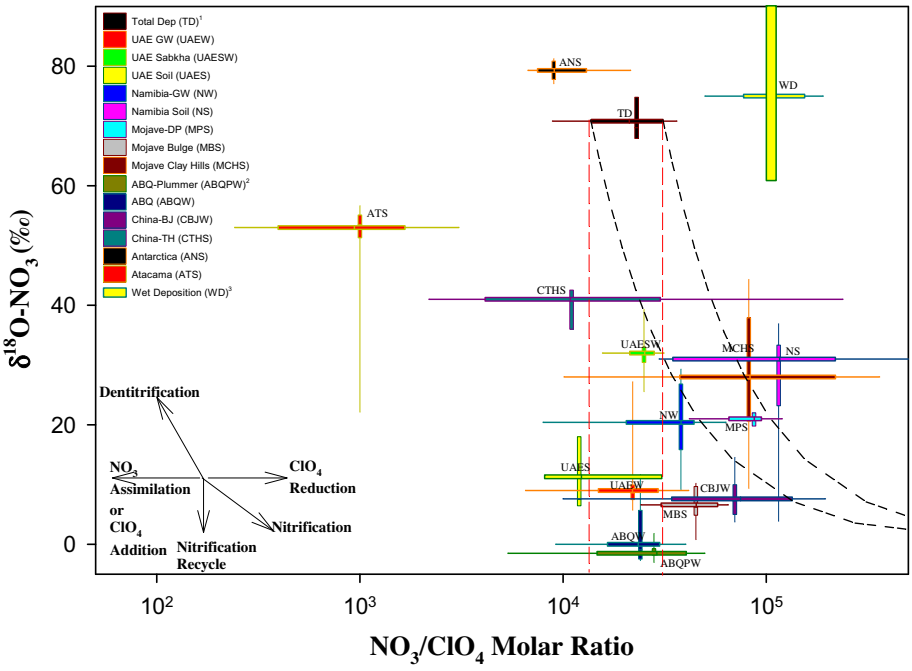

Fig. 8. Relation between $\delta^{18}O$ of NO_3^- and bulk NO_3/ClO_4 ratios in soils and groundwaters from arid and semi-arid locations as well as wet and dry deposition in North America. Box plots represent the 25th and 75th percentile values and extended lines from boxes represent the 90th and 10th percentiles. Dashed curves originating at total deposition indicate hypothetical trends caused by either: 1 (red lines) atmospheric NO_3 assimilation, mineralization, and nitrification with no net loss or gain of N; or 2 (black curve) addition of biogenic NO_3^- to uncycled atmospheric NO_3, assuming in both cases ClO_4^- is unaffected. Arrows in the lower left corner indicate hypothetical qualitative trajectories that could be caused by various processes. ([1]Andraski et al., 2014; [2]Plummer et al., 2006; [3]Rajagopalan et al., 2009).

fractionation effect of NO_3^- reduction, yielding local positive correlations between $\delta^{15}N$ and $\delta^{18}O$ at some sites. NO_3^- reduction can occur in the unsaturated zone and/or in groundwater after recharge. In addition, minor variations in $\delta^{18}O$ of biogenic NO_3^- may be related to local $\delta^{18}O$ of meteoric water during nitrification, and N cycling in soils and plants can cause local or regional variation in the $\delta^{15}N$ values of organic matter that is subject to nitrification (Handley et al., 1999; Amundson et al., 2003; McMahon and Böhlke, 2006). Isotopic variations caused by N cycling and NO_3^- reduction effects appear to be most prevalent at sites with relatively large fractions of biogenic NO_3^-, such that the combined effects of these major processes give a roughly triangular shape to the collection of isotope data in Fig. 6 with the exception of Antarctica, which has anomalously low $\delta^{15}N$.

Clearly, patterns and processes are complex and each site is unique. Nevertheless, to facilitate discussion of individual sites and sample types, we present the following conceptual model relating relative concentrations of ClO_4^- and NO_3^- with the isotopic indicators of NO_3^- sources, based on the assumption that atmospheric sources ultimately are important for both ClO_4^- and NO_3^-. Assuming no net gains or losses of ClO_4^- other than atmospheric deposition, relations between NO_3^-/ClO_4^- ratios and NO_3^- $\delta^{18}O$ values can be explored using a mixing model with three bounding cases (Fig. 8): (1) deposition and preservation of atmospheric NO_3^- with no addition of biogenic NO_3^-; (2) preservation of atmospheric NO_3^- with addition of biogenic NO_3^- produced by nitrification of reduced N from either fixed N_2, atmospheric NH_4^+, or accumulated organic matter (Fig. 8 black dashed lines); and (3) assimilation of atmospheric NO_3^- and regeneration with biogenic NO_3^- with no net gain or loss of N (Fig. 8 red dashed lines). In this model, we have excluded the case of significant simultaneous NO_3^- and ClO_4^- reduction or NO_3^- reduction alone, which are alternative possibilities discussed below. For the Mojave and Atacama sites, ClO_4^- stable isotope data can be used to exclude large amounts of biological reduction (Jackson et al., 2010). We have not ruled out the possibility of abiotic O exchange with H_2O as an alternative to nitrification as a way of lowering $\delta^{18}O$ of atmospheric NO_3^-, but there is no direct evidence for such exchange in these environments, whereas there is evidence that lower NO_3^- $\delta^{18}O$ values are associated with increasing soil biologic activity.

3.2. Groundwater results

3.2.1. Groundwater overview

The ClO_4^- concentrations in groundwater samples varied over four orders of magnitude, whereas the NO_3^-/ClO_4^- molar ratios were remarkably constant (average = 24,000) and almost identical to that of total atmospheric deposition in the Amargosa Desert (Fig. 2). This is true despite the geographic diversity of arid and semi-arid locations and isotopic evidence for varying degrees of biologic N cycling

in soils or plants prior to recharge at these sites (Fig. 6 and 8). Isotopic evidence for varying NO_3^- reduction in groundwater was not associated with substantial variation of NO_3^-/ClO_4^- ratios. However, it should be noted that the variation in NO_3^-/ClO_4^- ratios within most sites could be sufficient to accommodate substantial (>50%) NO_3^- losses. Cl^-/ClO_4^- ratios were much more variable and for most sites these constituents were not correlated (Fig. 2; Table 1). The lack of correlation and much larger Cl^-/ClO_4^- ratios compared to total deposition for non-coastal sites supports addition of Cl^- from non-atmospheric sources, "episodic Cl^-" or "non-co-deposited Cl^-" in many cases.

3.2.2. Albuquerque basin, U.S. (ABQ)

ClO_4^- concentrations in ABQ groundwater samples ($n = 63$) varied over a relatively narrow range (<0.05 ($n = 22$) to 3.1 μg/L) and concentrations were similar to those previously reported for this aquifer system (Plummer et al., 2006) (Fig. 4). While some wells may have been influenced by anthropogenic activities, many were not impacted based on groundwater ages (Plummer et al., 2006; Bexfield et al., 2011). For the 41 samples with detectable ClO_4^-, NO_3^- and ClO_4^- were correlated ($r = 0.82$) but there was no correlation between Cl^- and either ClO_4^- or NO_3^- ($r = 0.22$ and 0.05, respectively) (Table 1 and Fig. 4). The average NO_3^-/ClO_4^- and Cl/ClO_4^- molar ratios were 22,000 and 300,000, respectively.

A subset ($n = 30$) of ABQ groundwater samples was also evaluated for NO_3^- stable isotopic composition ($\delta^{15}N$ and $\delta^{18}O$) (Bexfield et al., 2011). NO_3^- in the aquifer appears to be almost completely biogenic and NO_3^- in a number of wells may have been impacted by denitrification given the linear trend, correlation ($r = 0.90$) and slope (1.05) of some $\delta^{15}N$ and $\delta^{18}O$ data pairs (Fig. 6) (Granger et al., 2008). These results are consistent with previous findings (Plummer et al., 2006). NO_3^- stable isotope data were available for 9 of the 22 samples with ClO_4^- concentrations below the reporting limit (0.05 μg/L). Of these, the $\delta^{15}N$ and $\delta^{18}O$ values of all but one exhibited evidence of denitrification. These data could indicate ClO_4^- reduction was associated with partial NO_3^- reduction in some parts of the system. For water samples ($n = 21$) with detectable ClO_4^- and NO_3^-, and with NO_3^- stable isotope data, $\delta^{18}O$ values of NO_3^- were relatively low (<1‰ for all but 2 samples) and there was no apparent relation between NO_3^-/ClO_4^- molar ratios and $\delta^{18}O$ or $\delta^{15}N$ values that would indicate substantial NO_3^- reduction or ClO_4^- reduction. Dissolved O_2 concentrations were highly variable (<0.1–7 mg/L) but there was no apparent relationship with NO_3^- or ClO_4^- concentrations. Jackson et al. (2010) reported similar NO_3^- isotopic composition ($\delta^{18}O$ ~−1‰) and NO_3^-/ClO_4^- ratios (18,000 and 28,000) for two oxic groundwater samples from the ABQ basin.

NO_3^-/ClO_4^- ratios and NO_3^- stable isotopic compositions of ABQ groundwaters are consistent with a model of atmospheric deposition and subsequent recycling of NO_3^- with no net addition of NO_3^- (Fig. 8), but with substantial addition of Cl^- (Fig. 7). The source of the Cl^- could originally be from non-atmospheric sources, "episodic Cl^-", or "non-co-deposited Cl^-" (as previously defined). For the "episodic Cl^-" case, NO_3^- and ClO_4^- would have to have been reduced substantially (~2 orders of magnitude), which is not supported by available isotope data for NO_3^- (Fig. 6) or ClO_4^- (Jackson et al., 2010).

3.2.3. Edwards Aquifer, U.S

ClO_4^- concentrations in Edwards Aquifer samples ($n = 92$) varied over a narrow range (<0.05 ($n = 2$) to 1.0 μg/L). No information is available regarding the source of the ClO_4^- in this system and it is possible that some groundwater is impacted by anthropogenic NO_3^- and ClO_4^-. NO_3^- and ClO_4^- were marginally correlated ($r = 0.22$), as were Cl^- and ClO_4^- ($r = 0.27$) but no significant relation exists between Cl^- and NO_3^- (Table 1 and Fig. 4). The average NO_3^-/ClO_4^- molar ratio (22,000) was the same as that for the ABQ basin, but the average Cl^-/ClO_4^- molar ratio (96,000) was less than that for the ABQ basin. The stable isotopic compositions of NO_3^- are not available for samples evaluated for ClO_4^- concentrations. Other studies have evaluated the stable isotopic composition of NO_3^- in the same segment of the Edwards Aquifer and concluded that the NO_3^- is predominately biogenic with no evidence of denitrification based on either the isotope data or excess N_2 gas (Musgrove et al., 2010). Similar to the ABQ basin, the data could be consistent with a model in which atmospheric NO_3^- deposition largely was replaced by biogenic NO_3^- in recharge with no net loss or gain, and with addition of Cl^- (~10×) from sources other than atmospheric co-deposition (Fig. 7).

3.2.4. Loess Plateau, China

ClO_4^- concentrations in Loess Plateau groundwater samples ($n = 10$) varied over a range (0.6–1.6 μg/L) similar to those for the ABQ basin and Edwards Aquifer (Fig. 4). NO_3^- and ClO_4^- concentrations were correlated ($r = 0.95$) but Cl^- was not correlated with either ClO_4^- or NO_3^- (Table 1). The NO_3^-/ClO_4^- and Cl^-/ClO_4^- molar ratios were the lowest of any groundwater evaluated (~11,000 and 47,000, respectively). No data are available concerning the age of the groundwater or the origin of the NO_3^- but the NO_3^-/ClO_4^- ratios are less and Cl^-/ClO_4^- ratios greater than in measured deposition (Figs. 2 and 7). Although agriculture was a common land use in the region, sampled groundwater was not highly enriched in NO_3^-. Irrigation was almost absent in the area. It is not possible to discuss the origin or subsequent fate of NO_3^- due to the absence of NO_3^- isotope data, but the relation between NO_3^- and ClO_4^- is similar to that in other geographically distant sites.

3.2.5. Badain Jaran, China

ClO_4^- concentrations in groundwater samples ($n = 20$) ranged from 0.3 to 2.1 μg/L and were correlated with NO_3^- ($r = 0.57$) (Fig. 4, Table 1) but Cl^- was not correlated with ClO_4^- or NO_3^-. The average NO_3^-/ClO_4^- molar ratio (61,000) was the highest of any of the groundwater locations. Given the remoteness of the location, lack of intensive agriculture, and age of at least some of the groundwater evaluated, it is likely the ClO_4^- is indigenous (Gates et al., 2008a,b). NO_3^- in this system previously has

been attributed to nitrification of NH_4^+ derived from atmospheric deposition or from mineralization of organic matter produced by nitrogen fixation or biologic assimilation of atmospheric N. In a few samples, NO_3^- may have been partially reduced through denitrification and a few samples with elevated $\delta^{18}O$ and low $\delta^{15}N$ of NO_3^- may have minor unaltered atmospheric components (Gates et al., 2008a). Our samples represent a subset of those analyzed by Gates et al. (2008a). Of the 20 samples we evaluated for ClO_4^-, NO_3^- stable isotope data were available for 10 (Fig. 6). Six samples previously identified as most likely to contain NO_3^- impacted by denitrification have NO_3^-/ClO_4^- molar ratios that are not significantly lower than the overall average (i.e., do not appear to indicate substantial preferential NO_3^- loss). Three samples appear to be impacted by denitrification based on relatively low NO_3^-/Cl^- ratios and elevated $\delta^{15}N$ and $\delta^{18}O$ values (Gates et al., 2008a). However, even for these samples the ratio of NO_3^-/ClO_4^- is not consistently lower than the overall average.

NO_3^- and ClO_4^- occurrence are consistent with atmospheric deposition and at least partial preservation of the atmospheric NO_3^- with substantial dilution (replacement and addition) by biogenic NO_3^- based on slightly elevated $\delta^{18}O$ and elevated NO_3^-/ClO_4^- ratios (Fig. 8). Cl^-/ClO_4^- and Cl^-/NO_3^- ratios support large (~100×) inputs of local, "episodic", or "non-co-deposited atmospheric Cl^-", similar to the ABQ aquifer (Fig. 7).

3.2.6. Namibia

ClO_4^- concentrations in Namibia groundwater samples ($n = 10$) ranged from 2.7–97 μg/L (Fig. 4). ClO_4^- was correlated with NO_3^- and Cl^- ($r = 0.91$ and 0.89, respectively) and as such NO_3^- and Cl^- were also correlated ($r = 0.96$) (Table 1). Given the remote location of the sample sites, high concentrations of ClO_4^- and NO_3^-, and NO_3^- isotopic composition, the ClO_4^- and NO_3^- are considered to be natural. The average NO_3^-/ClO_4^- ratio (29,000) was similar to those in all other groundwaters evaluated excluding the Badain Jaran, while the average Cl^-/ClO_4^- molar ratio was much higher (2,300,000). Stable isotope data indicate NO_3^- in the Namibia samples was predominantly biogenic, but included substantial unaltered atmospheric components based on elevated $\Delta^{17}O$ values in some samples (1.1–5.9‰; $n = 5$). The NO_3^- also appears to have been variably affected by NO_3^- reduction based on elevated $\delta^{18}O$ and $\delta^{15}N$ values (Fig. 6) and higher $\delta^{18}O$ values than expected from biogenic-atmospheric mixtures based on the $\Delta^{17}O$ values.

Factors affecting the Namibia groundwater could be similar to those at the Badain Jaran site (atmospheric deposition with conservation of the atmospheric component and dilution by biogenic NO_3^-) but altered by some denitrification (Fig. 8). High Cl^-/ClO_4^- ratios could be due to high local Cl^- deposition fluxes considering the coastal proximity, as values overlap with the high end of the range for wet deposition from US coastal locations. This is supported by the significant correlation between Cl^- and ClO_4^- for this site but not others, and by the similar Cl^-/ClO_4^- ratios in surface soils (Fig. 7).

3.2.7. UAE

Maximum ClO_4^- concentrations for UAE groundwater were the highest of any groundwater evaluated (Fig. 4). Highest concentrations (500–740 μg/L) occurred in sabkha areas ($n = 5$) but concentrations in some inland fresh groundwater ($n = 20$) were also elevated (0.1–108 μg/L), similar to the concentration range for Namibia groundwater. ClO_4^- and NO_3^- were well correlated with each other ($r = 0.98$) and with Cl^- (Table 1). The average NO_3^-/ClO_4^- molar ratio (22,000) was similar to those for the Edwards, ABQ, and Namibia sites (22,000, 23,000, and 29,000, respectively) (Table 1). The NO_3^- in most ($n = 10$) of the fresh-water samples (production wells) for which NO_3^- stable isotope data are available ($n = 12$) appears to be predominantly biogenic, with little evidence of NO_3^- reduction ($\delta^{15}N$ ~2–6‰ and $\delta^{18}O$ ~5–10‰; Fig. 6). In contrast, all of the sabkha locations and two of the fresh-water well samples had a substantial unaltered atmospheric component with variable impacts from NO_3^- reduction based on $\delta^{18}O$ and $\delta^{15}N$ of NO_3^- (Fig. 6) as well as $\Delta^{17}O$ of NO_3^- (8–8.5‰) in a subset of the sabkha samples

The sabkha data are consistent with evapo-concentration of deposition with some dilution by biogenic NO_3^- and only limited loss of the atmospheric NO_3^- component if the impact of NO_3^- reduction indicated by isotope data is taken into account. Cl^-/ClO_4^- ratios were elevated and variable, possibly reflecting variable marine, atmospheric, and subsurface salt sources, and are generally similar to Namibia groundwater values, consistent with the coastal location and correlation between Cl^- and ClO_4^- (Table 1, Fig. 7). UAE non-sabkha groundwater is more consistent with NO_3^- cycling rather than simple dilution (addition only) by biogenic NO_3^-. Cl^-/ClO_4^- ratios are similar to sabkha samples but much higher than for UAE surface soil samples (see below) suggesting that atmospheric deposition may not be the dominant source of the Cl^-.

3.3. Soil and caliche results

3.3.1. Soil and caliche overview

ClO_4^- concentrations in soils/caliches for all sites vary over a larger range (0.1–10^6 μg/kg) than those in groundwater (Figs. 2 and 3). Similarly, NO_3^-/ClO_4^- ratios appear to be more variable in soils/caliches than in groundwater (Figs. 2 and 3). In part, these contrasts may be related to the fact that soil/caliche samples are likely to exhibit local heterogeneity caused by selective crystallization, re-dissolution, and redistribution of salts during infiltration, whereas groundwater is more likely to represent spatially and temporally integrated samples of infiltrated salts. Nonetheless, there are clear relations between soil and groundwater NO_3^- and ClO_4^- concentrations within sites and between sites

Overall there appear to be major groupings of NO_3^-/ClO_4^- molar ratios that include 1) Mojave soil/caliche (85,000) and southern Africa soil (120,000); 2) all groundwater (24,000) and UAE soil (21,000); 3) Antarctica soil (14,000) and China Turpan-Hami soil/caliche (12,000); and 4) Atacama soils/caliches (1400) (Fig. 7). The first group (Mojave and southern Africa soil) ratios are similar

to the average ratio (~100,000) in wet deposition (Rajagopalan et al., 2009). The ratios of the second group (all groundwaters and UAE soil) are essentially identical to the ratio in total deposition at the Amargosa Desert Research Site (22,000) (Andraski et al., 2014). Ratios in the third group (Antarctica and Turpan-Hami) are lower but still similar to that in total atmospheric deposition, while the Atacama ratio is an order of magnitude lower and unique. The last two groups, with the lowest NO_3^-/ClO_4^- ratios, are also the most arid. Soil Cl^-/ClO_4^- ratios are much more variable than NO_3^-/ClO_4^- ratios, as in the groundwater sample sets; only the Antarctica and Atacama soil data sets exhibit a clear relation between Cl^- and ClO_4^-. Each site is discussed below in more detail in order of the major groupings and generally from more biologically active to less biologically active.

3.3.2. Mojave Desert

Soil samples were collected from three different environments (surface of clay hills, valley floor desert pavement, and deep sub-surface salt bulge), all in a relatively small but geographically diverse area of the Mojave Desert (Fig. 1). These samples do not represent "typical" soils but rather were chosen for their known accumulations of salts. Concentrations of ClO_4^- in these samples ranged from a low of 0.1 μg/kg (salt bulge) to a high of 5500 μg/kg (Confidence Hills) (Fig. 5). Samples (0–1 m) from the clay hills of southern Death Valley (Confidence Hills, Bully Hill, and Saratoga Hills) had the highest known concentrations of indigenous ClO_4^- in the U.S., and were similar to those described in previous studies (Jackson et al., 2010; Lydbrand et al., 2013). Discrete-depth samples from a subsurface salt bulge had a wide range of ClO_4^- concentrations (0.1–20 μg/kg), similar to other reported southwestern U.S. subsurface salt bulges (Rao et al., 2007). Near-surface samples from desert pavement on the Amargosa Desert valley floor contained concentrations of ClO_4^- similar to those in the nearby subsurface salt bulge. For comparison, a set ($n = 48$) of composite (0–30 cm) samples collected in a pre-defined grid covering a 0.1 km^2 hill-slope area of a nearby knoll was reported to have an average ClO_4^- concentration of 3.0 ± 2.6 μg/kg with a range of 0.8–11.8 μg/kg (Andraski et al., 2014).

ClO_4^- concentrations for all sites in the Mojave Desert are significantly correlated with NO_3^- ($r = 0.66$) but not with Cl^- ($r = 0.18$) (Table 2, Fig. 5). ClO_4^- and NO_3^- concentrations from individual profiles in and near the Death Valley clay hills were generally but not always significantly correlated. In addition, for the spatially varying desert pavement composite, desert pavement profile, and subsurface salt bulge, concentrations of ClO_4^- and NO_3^- were correlated ($r = 0.90$, 0.99, and 0.92, respectively). ClO_4^- was not correlated with Cl^- in the Mojave sample sets except for the subsurface salt bulge, desert pavement sites, and samples from Rainbow Hills. Cl^- and NO_3^- were also correlated for many of the same locations for which ClO_4^- and NO_3^- were correlated. A previous study found a significant but weaker relationship between NO_3^- and ClO_4^- in samples from the clay hills including some of the same locations reported here (Lybrand et al., 2013). One possible reason for the lower degree of correlation in the Lybrand study may have been the relatively high reportable ClO_4^- detection limit (165 μg/kg).

The molar ratios of NO_3^-/ClO_4^- for all Mojave locations varied from 25,000 to 240,000 with an overall average of 85,000 (Table 2). NO_3^-/ClO_4^- molar ratios were most variable in the clay hills samples, while the desert pavement and sub-surface salt bulge NO_3^-/ClO_4^- ratios were more uniform (40,000–86,000). These ratios are similar to those reported for other salt bulges in the arid southwestern U.S. (30,000–51,000, 27,000, and 218,000 for depth profiles from the Chihuahuan Desert, Amargosa Desert, and Yucca Flats, respectively) (Rao et al., 2007). Mojave Desert soil NO_3^-/ClO_4^- molar ratios are generally higher than the average ratio in total deposition at the Amargosa Desert Research Site (Andraski et al., 2014). The total deposition sample site was co-located with the desert pavement and sub-surface salt-bulge sites and within ~100 km of the remaining Mojave sites. In contrast to the relatively similar average NO_3^-/ClO_4^- ratios in Mojave sample sets, average Cl^-/ClO_4^- ratios varied over two orders of magnitude (77,000–7,400,000), indicating processes other than evapo-concentration affected anion ratios in the region.

Stable isotope data for NO_3^- ($\delta^{18}O$, $\Delta^{17}O$, and $\delta^{15}N$) in samples from the Death Valley clay hills and Rainbow Hills previously demonstrated that the NO_3^- is partially (20–50%) atmospheric in origin and partially biogenic, with no evidence of substantial isotope effects from NO_3^- reduction (Böhlke et al., 1997; Michalski et al., 2004; Jackson et al., 2010; Lybrand et al., 2013). NO_3^- in soil samples from Irwin Basin was mainly biogenic (Fig. 6) (Densmore and Böhlke, 2000). The $\delta^{18}O$ and $\delta^{15}N$ of NO_3^- in samples from the desert salt bulge support a largely biogenic source of NO_3^- while those in samples from near-by desert pavement appear to have a substantial (up to ~20%) atmospheric component (Fig. 6) (Andraski et al., 2014).

NO_3^-/ClO_4^- ratios and NO_3^- stable isotope ratios for samples from the Mojave clay hills are consistent with a model of atmospheric deposition and addition of biogenic NO_3^- without significant recycling (Fig. 8), and with substantial addition of Cl^- (Fig. 7) from "episodic Cl^-", "non-co-deposited Cl^-" sources or local non-atmospheric sources, consistent with the sedimentary host rocks and lack of plant life on the hills. Samples from the deep bulge are more similar to groundwater, indicating a largely recycled NO_3^- component consistent with N that infiltrated through the active soil zone. Samples of desert pavement are intermediate to the other two sample sets reflecting limited recycling of the atmospheric NO_3^- component and addition of biogenic NO_3^-.

The relatively low NO_3^-/ClO_4^- ratios in the salt bulge and groundwaters may indicate that soil processes tend to decrease NO_3^- relative to ClO_4^-. The decrease in the NO_3^-/ClO_4^- ratio could be due to episodic microbial reduction, though soils in these arid environments are generally well aerated. Another possibility could be uptake and assimilation of NO_3^- by plants and accumulation as organic N. A recent study suggested that while both ClO_4^- and NO_3^- are taken up by desert plants, the ClO_4^- can remain unprocessed and recycled back to the soils while NO_3^- is largely

fixed within the plant tissue (Andraski et al., 2014). The similar low NO_3^-/ClO_4^- ratio for groundwaters and deep salt bulge, given the complete loss of the original atmospheric NO_3^- component, suggests that in arid and semi-arid areas there is an upper limit to the amount of oxidized N that escapes from the biologically active vadose zone and that long term fluxes of NO_3^- may be somewhat regulated. Only in cases of extreme aridity or surface features (e.g. desert pavement), which limit infiltration, do ratios increase from NO_3^- addition in the relative absence of assimilation and gas loss.

3.3.3. Southern Africa

In contrast to the Mojave sample sites, southern Africa soil sample sites were not selected based on known salt accumulations. ClO_4^- concentrations varied from 0.2 to 45 μg/kg, with no relation to surface feature (pan, fan, or vertical profile) (Fig. 5). Samples from Botswana and South Africa playa surfaces were similar to those from Namibia. For both the Namibia and Botswana sites, as well as the combined data set, ClO_4^- and NO_3^- concentrations were correlated (Table 2, Fig. 5). Similar to the Mojave Desert samples, there were no significant correlations between Cl^- and ClO_4^- or Cl^- and NO_3^-. Average molar ratios of NO_3^-/ClO_4^- were similar for the three sites (96,000, 150,000, and 125,000) with an average ratio of 120,000 (Table 2), significantly greater than Namibia groundwater samples. Site average Cl^-/ClO_4^- ratios were much more variable (650,000–41,000,000). NO_3^- in the Namibia surface soils contained a greater unaltered atmospheric NO_3^- component (20–50%) than groundwater from Namibia (Fig. 6), and was intermediate to Mojave Desert pavement and clay hill samples (Fig. 8). NO_3^-/ClO_4^- ratios largely overlap with ratios of the Mojave Desert sample sets (e.g. clay hills and desert pavement) but are higher than ratios for Namibia groundwater (Fig. 8).

Overall, the Namibia soil data set appears to resemble the Mojave clay hills data set, consistent with a largely preserved atmospheric component with addition of biogenic NO_3^- (Fig. 8). While the unusually high Cl^-/ClO_4^- ratios in the Namibia samples could in part be due the coastal proximity, the lack of correlation between Cl^- and NO_3^- or ClO_4^- indicates local, "episodic", or "non-co-deposited Cl^-" sources may be important, similar to the Mojave Clay hills (Fig. 7).

3.3.4. UAE

Sample sites in the UAE represent both typical soil and sabkha sediment. Soil ClO_4^- concentrations ($n = 7$) ranged from < 0.1 ($n = 2$) to 13 μg/kg and those for sabkha sediment ($n = 7$) were generally higher ($<0.1 (n = 2)$ to 262 μg/kg). ClO_4^- and NO_3^- were correlated for both soil ($r = 0.87$) and sabkha sediments ($r = 0.97$) with an overall correlation coefficient of 0.99 (Table 2 and Fig. 5). Cl^- and ClO_4^- were not correlated, nor were NO_3^- and Cl^-. NO_3^-/ClO_4^- molar ratios were similar in soils and sabkha sediments (14,000 and 28,000, respectively), while Cl/ClO_4^- ratios were much more variable (19,000 and 1,700,000, respectively). Isotope data indicate the source of NO_3^- in the soil samples is mainly biogenic except for two samples that may have around 20–50% unaltered atmospheric NO_3^-, both of which had very low NO_3^- and ClO_4^- concentrations (Fig. 6). NO_3^- in the sabkha samples apparently had substantial fractions of unaltered atmospheric NO_3^- (approximately 20–50%), and it also exhibited isotopic evidence of NO_3^- reduction. NO_3^-/ClO_4^- molar ratios in UAE soil and sabkha samples were similar to those in UAE groundwater (22,000) and Amargosa Desert total deposition (22,000) (Fig. 8).

The NO_3^-/ClO_4^- ratios and NO_3^- isotopic compositions of the soil samples are consistent with substantial NO_3^- recycling, perhaps consistent with relatively high local precipitation, similar to UAE groundwater (Fig. 8). Sabkha samples are more consistent with biogenic addition and limited recycling, given the large unaltered atmospheric component and higher NO_3^-/ClO_4^- ratios and expected impact of NO_3^- reduction. Interestingly, UAE soil Cl/ClO_4^- ratios are near Mojave total deposition values and an order of magnitude lower than UAE groundwater values despite the similar NO_3^-/ClO_4^- ratios and proximity to the coast. The lack of correlation between soil Cl^- and ClO_4^-, but strong correlation for groundwater coupled with higher ClO_4^- concentrations in groundwater than soil, suggest that the groundwater Cl^-, NO_3^-, and ClO_4^- were not simply derived from concentrated infiltration but rather may indicate dissolution of stored salts in the subsurface or that the groundwater was not recharged locally.

3.3.5. China, Turpan-Hami

High concentrations of ClO_4^- (~100 to 16,000 μg/kg) were present in a relatively small set ($n = 11$) of samples from three sites in the vicinity of recently described massive NO_3^- deposits of northern China (Li et al., 2010; Qin et al., 2012). Concentrations of ClO_4^- were similar to those in the Mojave clay hills samples and ~1–2 orders of magnitude lower than the majority of samples from the Atacama NO_3^- deposits, even though the NO_3^- concentrations were similar between the Atacama and China deposits (Fig. 5). Turpan-Hami NO_3^- has been attributed largely to long-term atmospheric deposition, based on elevated $\Delta^{17}O$ (5–20‰) and $\delta^{18}O$ (30–60‰) values (Li et al., 2010; Qin et al., 2012), which are intermediate to NO_3^- from the Mojave clay hills and Atacama Desert. Previously reported ranges of $\delta^{18}O$ and $\Delta^{17}O$ indicate the Turpan-Hami NO_3^- is approximately 25–75% unaltered atmospheric. Data from the current study indicate similar atmospheric components (Fig. 6). NO_3^- and ClO_4^- were correlated ($r = 0.61$) but Cl^- and ClO_4^-, and Cl^- and NO_3^-, were not. Cl^- concentration varied relatively little, while NO_3^- and ClO_4^- concentrations varied over 2 orders of magnitude (Fig. 5). Molar ratios of NO_3^-/ClO_4^- were generally lower than ratios for the Mojave Desert sites and for Mojave total atmospheric deposition, but the overall average ratio was still ~1 order of magnitude greater than the Atacama ratio, although the ranges do overlap (Fig. 7).

Given the large unaltered atmospheric NO_3^- component and the relatively low NO_3^-/ClO_4^- ratio in the Turpan-Hami samples, it would appear that there has not been much net addition of biogenic NO_3^- (Fig. 8). Compared to the Mojave total deposition anion ratios and NO_3^- isotope

values, the Turpan-Hami data are consistent with partial recycling of the atmospheric NO_3^- component. However given the extreme aridity and lack of vegetation, an alternative explanation may be that the Mojave total deposition NO_3^-/ClO_4^- ratios do not represent Turpan-Hami deposition ratios. For example, a lower contribution from wet deposition with higher NO_3^-/ClO_4^- might reduce the total deposition NO_3^-/ClO_4^- ratio and thus allow for biogenic addition without recycling. Similar to the Mojave, there also appears to be a substantial component of Cl^- unrelated to co-deposited NO_3^- and ClO_4^- (Fig. 7).

3.3.6. Antarctica, University Valley

ClO_4^- concentrations varied over a relatively narrow range (50–500 μg/kg); variations with depth were similar in magnitude to variations among locations (Fig. 5). These concentrations are similar to those previously reported for University Valley and Beacon Valley (Kounaves et al., 2010). Concentrations were higher than those of surface soils from other sites, excluding the samples from the Mojave clay hills, Atacama, and China Turpan-Hami. Concentrations of NO_3^- and ClO_4^- were correlated ($r = 0.83$–0.99) in all profiles, as were concentrations of Cl^- with ClO_4^- ($r = 0.72$–0.99) and NO_3^- ($r = 0.64$–0.99) with the exception of profile 7 (Table 2). Average molar ratios were similar among sites 7900–20,000; 4600–10,000; and 0.34–0.87, for NO_3^-/ClO_4^-, Cl/ClO_4^-, and Cl/NO_3^- respectively. The NO_3^-/ClO_4^- molar ratios were similar to those of Turpan-Hami samples, but an order of magnitude higher than Atacama ratios. The Cl^-/NO_3^- molar ratios for the Antarctica sites were lower than for all other sites, but the Cl^-/ClO_4^- ratios for the Atacama sites were lower than those for University Valley (Fig. 7).

NO_3^- in soils from the McMurdo Dry Valley region of Antarctica previously has been attributed to atmospheric deposition with no biogenic component based on extremely high $\delta^{18}O$ (>70‰) and $\Delta^{17}O$ values (>29‰) (Michalski et al., 2005). NO_3^- in Antarctica soil samples analyzed in this study had a similar $\delta^{18}O$ range (76–84‰) (Fig. 6). This site represents the extreme end of low biological activity both due to the very few degree days above 0 °C as well as the limited precipitation. NO_3^- deposition in Antarctica is somewhat unique and NO_3^- can also be subject to a number of isotopically fractionating abiotic processes (e.g. photolysis and volatilization) on snow and ice (e.g. Grannas et al., 2007 and Frey et al., 2009). Our soil samples did not appear to exhibit anomalous concentration ratios or NO_3^- isotopic compositions that might reflect post-depositional transformations. The ratios of NO_3^-/ClO_4^- and Cl/ClO_4^-, and NO_3^- isotopic compositions, coupled with strong correlations among all three species, support an unaltered atmospheric source consistent with the cold hyper-arid conditions and almost complete lack of biological activity (Fig. 8).

3.3.7. Atacama

ClO_4^- concentrations ($n = 102$) in Atacama soil/caliche samples ranged from a minimum of 0.5 μg/kg to a maximum of 1×10^6 μg/kg (Fig. 5). The vast majority of profile samples (AT) collected in the central depression contained ClO_4^- at concentrations that exceed those for all other sites evaluated in this study. Surface soil composites acquired along an east–west elevation transect varied in concentration; approximately 50% of the samples (those located above 2500 m elevation, east of the central depression and absolute desert where vegetation is present) had concentrations similar to those for the Mojave, southern Africa, and UAE sites. Spatial location (both altitude and geographic coordinates) is likely an important determinant of ClO_4^- concentration due to rainfall and evapotranspiration effects, but the associated discussion is beyond the scope of this paper.

For all profiles, surface composites, and the combined data set, NO_3^- and ClO_4^- were correlated except for the mine samples (Table 2). In general, correlation coefficients were lower for the relation between Cl^- and ClO_4^- compared to NO_3^- and ClO_4^- but still generally significant, and as such NO_3^- and Cl^- were generally correlated. NO_3^-/ClO_4^- molar ratios (550–2200) were at least an order of magnitude lower than at other sites evaluated in this study, with one exception (site AT16, where $NO_3^-/ClO_4^- = 13{,}000$). All the Atacama NO_3^-/ClO_4^- ratios were below the minimum ratios reported for wet and total deposition in North America (Rajagopalan et al., 2009; Andraski et al., 2014). Previous studies indicate the source of NO_3^- in the Atacama caliche deposits is largely atmospheric (>50%) (Böhlke et al., 1997; Michalski et al., 2004) and the stable isotopic compositions of samples evaluated in this study generally were consistent with this, except for a few of the surface soil composites far from the central depression in which NO_3^- appears to be mainly biogenic (Fig. 6). Cl^-/ClO_4^- molar ratios for the Atacama sites were similar to each other in magnitude and variability (615–4700) and were lower than at other sites evaluated in this study (Table 2).

The Atacama Desert is the location with the longest record of aridity and the most extreme aridity under present conditions, and this is reflected by the predominantly atmospheric source of NO_3^- with only limited biogenic NO_3^- (Böhlke et al., 1997; Michalski et al., 2004). The average Atacama soil NO_3^-/ClO_4^- ratio is at least one order of magnitude lower than all other measured deposition, soil/caliche, and groundwater ratios (Fig. 8). We exclude the possibility that the low ratio compared to other sites was caused by loss of ClO_4^- at all other sites based on the stable isotopic composition of ClO_4^- in the Mojave (Jackson et al., 2010) as well as other unpublished data for Antarctica and Turpan-Hami. There was also limited or no evidence for biological NO_3^- reduction in most of the sites studied. The low ratio is not likely caused by net loss of NO_3^- by denitrification or plant assimilation, given the hyper-arid conditions. The low ratio could be due to regionally low NO_3^- deposition flux or high ClO_4^- deposition flux. Both of these species are considered to be at least partly atmospheric in origin based on elevated $\Delta^{17}O$ values as well as ^{36}Cl content of ClO_4^- (Bao and Gu, 2004; Michalski et al., 2004; Sturchio et al., 2009; Jackson et al., 2010). Regionally low NO_3^- production does not seem likely as the overall average Cl^-/NO_3^- molar ratio (1.1) is the fourth lowest of all locations and matches reasonably well with

reported deposition ratios for the Atacama (0.74) (Ewing et al., 2006). An anomaly in the deposition flux of ClO_4^- presumably would require a mechanism to localize atmospheric production, as other sites in the southern hemisphere do not have such low NO_3^-/ClO_4^- ratios. Atacama ClO_4^- has a unique isotopic composition compared to other reported natural ClO_4^- from Mojave, Rio Grande Basin, and Southern High Plains (Böhlke et al., 2005; Jackson et al., 2010; Sturchio et al., 2011). The unique isotopic composition (low $\delta^{37}Cl$, $\delta^{18}O$, and $^{36}Cl/Cl$) could be related to an additional unknown production mechanism which could also explain the very low ratios of NO_3^-/ClO_4^-. Alternatively, given the duration of hyper-arid conditions in the Atacama (>2 million years), the relative enrichment and unique isotopic composition of ClO_4^- could be a reflection of atmospheric conditions that are no longer present. The age of the ClO_4^- in the Atacama has been estimated to be at least 750,000 years for the youngest samples, with a mean age of 3–8 million years based on $^{36}Cl/Cl^-$ ratios in ClO_4^- (Sturchio et al., 2009). This suggests that almost all of the Atacama ClO_4^- is older than 300,000 years, and thus predates the estimated time period over which ClO_4^- was deposited at other terrestrial locations.

3.4. Implications of $Cl^-/NO_3^-/ClO_4^-$ global correlations

The global consistency of NO_3^-/ClO_4^- ratios in all locations other than the Atacama is in contrast to the more variable Cl^-/NO_3^- and Cl^-/ClO_4^- ratios (Fig. 7). Cl^-/NO_3^- ratios are commonly used to evaluate N and/or NO_3^- gains/losses in various ecosystems. Co-variation of Cl^-/NO_3^- and Cl^-/ClO_4^- ratios illustrated in Fig. 7 indicates large variations in Cl^- are related to processes that either (1) do not affect NO_3^- or ClO_4^-, or (2) affect both NO_3^- and ClO_4^- similarly. Atmospheric deposition plots at the low end of the correlated data array in Fig. 7, indicating that many soils, caliches, unsaturated salt bulges, and groundwaters in arid and semi-arid regions have NO_3^-/ClO_4^- ratios similar to atmospheric deposition ratios, whereas Cl^-/NO_3^- and Cl^-/ClO_4^- ratios of terrestrial samples are systematically higher than deposition ratios. For the deposition data summarized in this paper (U.S. wet deposition (WD) and Mojave total deposition (TD)), the Cl^-/NO_3^- molar ratios (0.33 and 0.61 for WD and TD, respectively) are similar to that previously estimated from oxic groundwater data for the Middle Rio Grande Basin ($Cl^-/NO_3^- = 0.27$) (Plummer et al., 2006) as well as that calculated using reported data (2000–2010) for total deposition from 95 sites across the U.S. ($Cl^-/NO_3^- = 0.29$; $n = 892$) (CASTNET, 2014).

Cl^- concentrations in atmospheric deposition can vary independently of the concentrations of constituents with atmospheric sources. For example, Rajagopalan et al. (2006) reported mean values of Cl^-/NO_3^- and Cl^-/ClO_4^- in wet deposition at different sites across the U.S. varied by 2 orders of magnitude and much of the variation was related to distance from the coast, presumably reflecting variation in the sea-salt component relative to other components of the Cl^- deposition. Similarly, continental-scale studies of $^{36}Cl/Cl$ ratios in pre-anthropogenic groundwater in the U.S. and modern atmospheric deposition in Europe indicated maximum coastal marine Cl^- enrichment factors on the order of 20–40 (Davis et al., 2003; Johnston and McDermott, 2008). Varying deposition ratios could account for some of the regional terrestrial variation illustrated in Fig. 7, but probably not all of it, and presumably would not cause almost all terrestrial samples to be relatively enriched in Cl^-. The Cl^-/NO_3^- ratios of soil/caliche and groundwater samples vary over 3 orders of magnitude, with little relation to distance from the coast, although some of the highest Cl^-/NO_3^- ratios are from areas near coasts (e.g., Namibia and UAE). The highest wet deposition Cl^-/NO_3^- ratio observed by Rajagopalan et al. (2006) for 4 coastal sites (<50 km) was 17 (Puerto Rico) while the other 3 coastal sites had ratios < 4.

The array of data extending from atmospheric deposition toward higher Cl^-/NO_3^- and Cl^-/ClO_4^- ratios (Fig. 7), and the lack of a relation between the increase in Cl^-/NO_3^- ratio and the NO_3^-/ClO_4^- ratio (Fig. 7) suggests that either Cl^- at most sites has been supplemented by sources unrelated to the source of the original co-deposited NO_3^- or ClO_4^-, or that both NO_3^- and ClO_4^- were equally lost in these systems as previously described. Partial microbial reduction of NO_3^- is supported by isotope data at some sites (Fig. 6). However, NO_3^- isotopes at most sites appear to be relatively unfractionated and some indicate substantial unaltered atmospheric NO_3^-. For ClO_4^- and NO_3^- to be lost due to episodic reduction without apparent isotope effect would require complete loss at micro-sites and as much as 99% total loss to account for the magnitude of change in the Cl^-/NO_3^- ratios, which is considered improbable given the current aridity of most locations in this study. However, as previously mentioned, it is possible that some sites with elevated Cl^- concentrations contain atmospheric Cl^- that accumulated during previous wetter periods that supported biological reduction of NO_3^- and ClO_4^- (non-co-deposited Cl^-).

Another possible confounding factor may be the potential de-coupling of Cl^- and NO_3^- or ClO_4^- transport. Local redistribution of salts by selective crystallization, dissolution, and infiltration might have separated NO_3^- and ClO_4^- from Cl^- at the scale of individual samples or vertical profiles. Also, we have observed that at least some plants uptake ClO_4^- and NO_3^- proportionally while excluding Cl^- (Andraski et al., 2014). Biologic assimilation could be responsible for substantial N sequestration in persistent organic matter, and release of N gases (e.g., NH_3, N_2O, N_2) during remineralization, nitrification, or denitrification, could also lead to elevated Cl^-/NO_3^- ratios in soils and recharging groundwaters, but existing data do not support similar losses of ClO_4^- due to plant uptake (Tan et al., 2004b, 2006; Andraski et al., 2014). It is emphasized that the Atacama Desert occupies a unique position in all of the figures that present data from this study, which can only be achieved by assuming a localized *in-situ* production mechanism or unknown variation in the deposition ratios over million-year time scales that would not be recorded at the other sites.

4. CONCLUSIONS

ClO_4^- is globally distributed in soil and groundwater in arid and semi-arid regions on Earth at concentrations

ranging from 10^{-1} to 10^{6} μg/kg. Generally, the ClO_4^- concentration in these regions increases with aridity index, but also depends on the duration of arid conditions. In many arid and semi-arid areas, NO_3^- and ClO_4^- co-occur at consistent ratios (NO_3^-/ClO_4^-) that vary between $\sim10^4$ and $\sim10^5$. These ratios are largely preserved in hyper-arid areas that support little or no biological activity (e.g. plants or bacteria), but can be altered in areas with more active biological processes including N_2 fixation, N mineralization, nitrification, denitrification, and microbial ClO_4^- reduction. At first approximation, relatively constant NO_3^-/ClO_4^- ratios in desert environments are consistent with global atmospheric sources, and with dry deposition as a major controlling factor.

In contrast, much larger ranges of Cl^-/ClO_4^- and Cl^-/NO_3^- ratios indicate Cl^- varies independently from both ClO_4^- and NO_3^-. This is likely due to variation of sea salt Cl^- in deposition, plus variable addition of Cl^- from dust or subsurface sedimentary and evaporitic sources, and possibly excess Cl^- accumulation during past wetter periods of NO_3^- and ClO_4^- reduction. The general lack of correlation between Cl^- and ClO_4^- or NO_3^- implies that Cl^- is not a good indicator of co-deposition and should be used with care when interpreting oxyanion cycling and mass balances in arid systems.

In general, the co-occurrence of ClO_4^- and NO_3^- in arid and semi-arid locations, and associated variations in the isotopic composition of the NO_3^-, are consistent with a conceptual model of atmospheric origin, global co-deposition, and variable alteration of the NO_3^- pool by biogenic addition, assimilation, and/or recycling on the surface. Preservation of the atmospheric deposition NO_3^-/ClO_4^- ratio in unsaturated-zone accumulations and groundwater in areas where biological activity is substantial and on-going appears to indicate limits to net gains and losses of N through biological processes in soils between deposition inputs and infiltration outputs.

Measurements of ClO_4^- concentration in desert regions could be useful for interpreting major anion cycles and processes, particularly with respect to the less-conserved NO_3^- pool. If more accurate local measures of deposition can be obtained, then ClO_4^- surface accumulations in conjunction with NO_3^- isotopic composition could be useful in evaluating the duration of arid conditions that led to such accumulations, and potentially also the extent of biological processes and nitrogen mass transfers.

The Atacama Desert appears to be unique compared to other arid and semi-arid locations. There, exceptional enrichment in ClO_4^- compared to Cl^- or NO_3^-, accompanied by unique ClO_4^- isotopic characteristics (Bao and Gu, 2004; Böhlke et al., 2005; Jackson et al., 2010), may reflect an unusually efficient, but yet unknown, *in-situ* production mechanism, regionally elevated atmospheric ClO_4^- production rates, or higher ClO_4^- production rates in pre-Pleistocene times.

In the absence of microbial reduction, ClO_4^- can persist in many environmental conditions. On early Earth, prior to the onset of microbial ClO_4^- reduction, ClO_4^- concentrations could have been much higher than currently observed. However, the net impact of microbial ClO_4^- reduction on the global chlorine biogeochemical cycle remains unconstrained.

Elevated concentrations of ClO_4^- reported on the surface of Mars, and its enrichment with respect to Cl^- and NO_3^-, could reveal important clues regarding the climatic, hydrologic, and potentially biologic evolution of the planet. Given the highly conserved ratio of NO_3/ClO_4^- in non-biologically active areas on Earth, it may be possible to use alterations of this ratio as a biomarker on Mars.

ACKNOWLEDGEMENTS

This work was supported by the Strategic Environmental Research and Development Program (SERDP Project ER-1435) of the U.S. Department of Defense; the U.S. Geological Survey Toxic Substances Hydrology Program, National Research Program, Groundwater Resources Program, and National Water Quality Assessment Program; the U.S. Antarctic Research Program[NSF]; and the Abu Dhabi Emirate National Drilling Company. CL acknowledges additional support from grants ICM P05-002 and PFB-23 to the IEB. We are also grateful to SQM for allowing access to a nitrate mine. We thank Dr. Peter McMahon, Dr. Hans Eggenkamp, and anonymous reviewers for insightful comments and suggestions on the manuscript. We thank J. Hannon and S. Mroczkowski for assistance with nitrate isotopic analyses. Any use of trade, product, or firm names is for descriptive purposes only and does not imply endorsement by the U.S. Government.

REFERENCES

Amundsen R., Austin A. T., Schuur E. A. G., Yoo K., Matzek V., Kendall C., Uebersax A., Brenner D. and Baisden W. T. (2003) Global patterns of the isotopic composition of soil and plant nitrogen. *Global Biogeochem. Cycles* **17**(1), 31-1 to 31-10.

Andraski B. J., Jackson W. A., Welborn T. L., Böhlke J. K., Sevanthi S. R. and Stonestrom D. A. (2014) Soil, plant, and terrain effects on natural perchlorate distribution in a desert landscape. *J. Environ. Qual.* **43**(3), 980–994.

Bao H. M. and Gu B. H. (2004) Natural perchlorate has a unique oxygen isotope signature. *Environ. Sci. Tech.* **38**, 5073–5077.

Bexfield L.M., Heywood C.E., Kauffman L.J., Rattray G.W. and Vogler E.T. (2011) Hydrogeologic setting and groundwater flow simulation of the Middle Rio Grande Basin regional study area, New Mexico, section 2 of Eberts, S.M., ed., Hydrologic settings and groundwater-flow simulations for regional investigations of the transport of anthropogenic and natural contaminants to public-supply wells—investigations begun in 2004: U.S. Geol. Surv. Prof. Paper, 1737-B, p. 2-1–2-61.

Böhlke J. K., Ericksen G. E. and Revesz K. (1997) Stable isotope evidence for an atmospheric origin of desert nitrate deposits in northern Chile and southern California, U.S.A. *Chem. Geol.* **136**, 135–152.

Böhlke J. K., Mroczkowski S. J. and Coplen T. B. (2003) Oxygen isotopes in nitrate: new reference materials for ^{18}O:^{17}O:16O measurements and observations on nitrate-water equilibration. *Rapid Com. Mass. Spec.* **17**, 1835–1846.

Böhlke J. K., Sturchio N. C., Gu B., Horita J., Brown G. M., Jackson W. A., Batista J. R. and Hatzinger P. B. (2005) Perchlorate isotope forensics. *Anal. Chem.* **77**, 7838–7842.

Bomar G. W. (1994) *Texas Weather*. University of Texas Press, Austin, TX, p. 287.

Casciotti K. L., Sigman D. M., Hastings M., Böhlke J. K. and Hilkert () Measurement of the oxygen isotopic composition of

nitrate in seawater and freshwater using the denitrifier method. *Anal. Chem.* **74**, 4905–4912.

Coates J. D. and Achenbach L. A. (2004) Microbial perchlorate reduction: rocket-fuelled metabolism. *Nat. Rev. Microbiol.* **2**, 569–580.

Coplen T. B., Böhlke J. K. and Casciotti K. L. (2004) Using dual bacterial denitrification to improve $\delta^{15}N$ determinations of nitrates containing mass independent ^{17}O. *Rapid Com. Mass Spec.* **18**, 245–250.

Davis S. N., Moysey S., Cecil L. D. and Zreda M. (2003) Chlorine-36 in groundwater of the United States: empirical data. *Hydrogeol. J.* **11**(2), 217–227.

Densmore J. N. and Böhlke J. K. (2000) Use of nitrogen isotopes to determine sources of nitrate contamination in two desert basins in California. interdisciplinary perspectives on drinking. *Water Risk Assess Manag.* **260**, 63–73.

Ericksen G.E. (1981) Geology and origin of the Chilean nitrate deposits. In *Geological Survey Professional Paper 1188*. Government Printing Office, Reston, VA.

Ericksen G. E., Hosterman J. W. and Amand St. (1988) Chemistry mineralogy, and origin of the clay-hill nitrate deposits Amaragosa River Valley, Death Valley region, California, U.S.A. *Chem. Geol.* **67**, 85–102.

Ewing S. A., Sutter B., Owen J., Nishiizumi K., Sharp W., Cliff S. S., Perry K., Dietrich W., McKay C. P. and Amundson R. (2006) A threshold in soil formation at Earth's arid-hyperarid transition. *Geochim. Cosmochim. Acta* **70**(21), 5293–5322.

Farhan Y. H. and Hatzinger P. B. (2009) Modeling the biodegradation kinetics of perchlorate in the presence of oxygen and nitrate as competing electron acceptors. *Biorem. J.* **13**, 65–78.

Frey M., Savarino J., Morin S., Erbland J. and Martins J. M. F. (2009) Photolysis imprint in the nitrate stable isotope signal in snow and atmosphere of East Antarctica and implications for reactive nitrogen cycling. *Atmos. Chem. Phys.* **9**, 8681–8696.

Gates J. B., Böhlke J. K. and Edmunds M. (2008a) Ecohydrological factors affecting nitrate concentrations in a phreatic desert aquifer in northwestern China. *Environ. Sci. Technol.* **42**, 3531–3537.

Gates J. B., Edmunds W. M., Darling W. G., Ma J., Pang Z. and Young A. A. (2008b) Conceptual model of recharge to southeastern Badain Jaran Desert groundwater and lakes from environmental tracers. *Appl. Geochem.* **23**, 3519–3534.

Gates J. B., Scanlon B. R., Mu X. and Zhang L. (2011) Impacts of soil conservation on groundwater recharge in the semi-arid Loess Plateau, China. *Hydrogeol. J.* **19**, 865–875.

Glavin D. P., Freissinet C., Miller K. E., Eigenbrode J. L., Brunner A. E. and Buch A., et al. (2013) Evidence for perchlorates and the origin of chlorinated hydrocarbons detected by SAM at the Rocknest aeolian deposit in Gale Crater. *J. Geophys. Res.: Planets* **118**(10), 1955–1973.

Granger J., Sigman D. M., Lehmann M. F. and Tortell P. D. (2008) Nitrogen and oxygen isotope fractionation during dissimilatory nitrate reduction by denitrifying bacteria. *Liminol. Oceanogr.* **53**, 2533–2545.

Grannas A. M., Jones A. E., Dibb J., Ammann M., Anastasio C., Beine H. J., Bergin M., Bottenheim J., Boxe C. S., Carver G., Chen G., Crawford J. H., Domine F., Frey M. M., Guzman M. I., Heard D. E., Helmig D., Hoffmann M. R., Honrath R. E., Huey L. G., Hutterli M., Jacobi H. W., Klan P., Lefer B., McConnell J., Plane J., Sander R., Savarino J., Shepson P. B., Simpson W. R., Sodeau J. R., von Glasow R., Weller R., Wolff E. W. and Zhu T. (2007) An overview of snow photochemistry: evidence, mechanisms and impacts. *Atmos. Chem. Phys.* **7**(16), 4329–4373.

Handley L. L., Austin A. T., Robinson D., Scrimgeour C. M., Raven J. A., Heaton T. H. E., Schmidt S. and Stewart G. R. (1999) The ^{15}N natural abundance ($d^{15}N$) of ecosystem samples reflects measures of water availability. *Aust. J. Plant Physiol.* **26**, 185–199.

Hannon J. E., Böhlke J. K. and Mroczkowski S. J. (2008) Effects of nitrate and water on the oxygen isotopic analysis of barium sulfate precipitated from solution. *Rapid Commun Mass Sp.* **22**, 4109–4120.

Hecht M. H., Kounaves S. P., Quinn R. C., West S. J., Young S. M. M., Ming D. W., Catling D. C., Clark B. C., Boynton W. V., Hoffman J., DeFlores L. P., Gospodinova K., Kapit J. and Smith P. H. (2009) Detection of perchlorate and the soluble chemistry of Martian soil at the Phoenix Lander Site. *Science* **325**, 64–67.

Jackson W. A., Joseph P., Laxman P., Tan K., Smith P. N., Yu L. and Anderson T. A. (2005) Perchlorate accumulation in forage and edible vegetation. *J. Agr. Food Chem.* **53**(2), 369–373.

Jackson W. A., Böhlke J. K., Gu B., Hatzinger P. B. and Sturchio N. C. (2010) Isotopic composition and origin of indigenous natural perchlorate and co-occurring nitrate in the southwestern United States. *Environ. Sci. Technol.* **44**, 4869–4876.

Jackson W. A., Davila A., Estrada N., Lyons W. B., Coates J. D. and Priscu J. (2012) Perchlorate and chlorate biogeochemistry in ice-covered lakes of the McMurdo Dry Valleys, Antarctica. *Geochet Cosmochim. Cosmochim. Acta.* **98**, 19–30.

Johnston V. E. and Dermott F. (2008) The distribution of Cl 36 in precipitation across Europe in spring 2007. *Earth Planet Sci. Lett.* **275**, 154–164.

Kannan K., Praamsma M. L., Oldi J. F., Kunisue T. and Sinha R. K. (2009) Occurrence of perchlorate in drinking water, groundwater, surface water and human saliva from India. *Chemosphere* **76**, 22–26.

Koterba M. T., Wilde F. D., and Lapham W. W. (1995) Groundwater data-collection protocols and procedures for the National Water-Quality Assessment Program—Collection and documentation of water-quality samples and related data. *U.S. Geological Survey Open-File Report*, 95–399, 113.

Kounaves S. P., Stroble S. T., Anderson R. M., Moore Q., Catling D. C., Douglas S., McKay C. P., Ming D. W., Smith P. H., Tamppari L. K. and Zent A. P. (2010) Discovery of natural perchlorate in the Antarctic Dry Valleys and its global implications. *Environ. Sci. Technol.* **44**, 2360–2364.

Li Y., Qin Y., Liu F., Kejun H. and Wan D. (2010) Discovery of mass independent oxygen isotope compositions in superscale nitrate mineral deposits from Turpan-Hami Basin, Xinjiang, China and it significance. *Acta Geol. Sinica* **84**, 1514–1519.

Liebensteiner M. G., Pinske M. W. H., Schaap P. J., Stams A. J. M. and Lomans B. P. (2013) Archaeal (per)chlorate reduction at high temperature: An interplay of biotic and abiotic reactions. *Science* **340**, 85–87.

Lybrand R. A., Michalski G., Grahm R. C. and Parker D. R. (2013) The geochemical associations of nitrate and naturally formed perchlorate in the Mojave Desert, California, USA. *Geochim. Cosmochim. Acta* **104**, 136–147.

McMahon P. B. and Böhlke J. K. (2006) Regional patterns in the isotopic composition of natural and anthropogenic nitrate in groundwater, High Plains, USA. *Environ. Sci. Technol.* **40**, 2965–2970.

Michalski G., Savarino J., Böhlke J. K. and Thiemens M. H. (2002) Determination of the total oxygen isotopic composition of nitrate and the calibration of a $\Delta^{17}O$ nitrate reference material. *Anal. Chem.* **74**, 4989–4993.

Michalski G., Böhlke J. K. and Thiemens M. (2004) Long-term atmospheric deposition as the source of nitrate and other salts in the Atacama Desert, Chile: new evidence from mass-independent oxygen isotopic composition. *Geochim. Cosmochim. Acta* **68**, 4023–4038.

Michalski G., Bockheim J. G., Kendall C. and Thiemens M. (2005) Isotopic composition of Antarctic Dry Valley nitrate: Implications for NO(y) sources and cycling in Antarctica. *Geophys. Res. Lett.* **32**, 13817.

Musgrove M., Fahlquist L., Houston N. A., Lindgren R. J., and Ging P. B. (2010) Geochemical evolution processes and water-quality observations based on results of the National Water-Quality Assessment Program in the San Antonio segment of the Edwards aquifer, 1996–2006. *U.S. Geological Survey Scientific Investigations Report* 2010–5129, 93.

Nozawa-Inoue M., Scow K. M. and Rolston D. E. (2005) Reduction of perchlorate and nitrate by microbial communities in vadose soil. *Appl. Environ. Microbiol.* **71**, 3928–3934.

Parker D. R., Seyfferth A. L. and Reese B. K. (2008) Perchlorate in groundwater: a synoptic survey of "pristine" sites in the conterminous United States. *Environ. Sci. Technol.* **42**, 1465–1471.

Pérez-Fodich A., Reich M., Álvarez F., Snyder G. T., Schoenberg R., Vargas G., Muramatsu Y. and Fehn U. (2014) Climate change and tectonic uplift triggered the formation of the Atacama Desert's giant nitrate deposits. *Geology*. http://dx.doi.org/10.1130/G34969.1.

Plummer L. N., Bexfield L. M., Anderholm S. K., Sanford W. E. and Busenberg E. (2004) Geochemical characterization of ground-water flow in the Santa Fe Group aquifer system, Middle Rio Grande Basin, New Mexico. U.S. Geological Survey, Water-Resour. Invest. Report 03-4131.

Plummer L. N., Böhlke J. K. and Doughten M. W. (2006) Perchlorate in Pleistocene and Holocene groundwater in north-central New Mexico. *Environ. Sci. Technol.* **39**, 4586–4593.

Qin Y., Li Y. H., Bao H. M., Liu F., Hou K. J., Wan D. F. and Zhang C. (2012) Massive atmospheric nitrate accumulation in a continental interior desert, northwestern China. *Geology* **40**(7), 623–626.

Quinones O., Oh J. E., Vanderford B., Kim J. H., Cho J. and Snyder S. A. (2007) Perchlorate assessment of the Nakdong and Yeongsan watersheds, Republic of Korea. *Environ. Toxicol. Chem.* **7**, 1349–1354.

Rajagopalan S., Anderson T. A., Fahlquist L., Rainwater K. A., Ridley M. and Jackson W. A. (2006) Widespread presence of naturally occurring perchlorate in High Plains of Texas and New Mexico. *Environ. Sci. Technol.* **40**, 3156–3162.

Rajagopalan S., Anderson T., Cox S., Harvey G., Cheng Q. and Jackson W. A. (2009) Perchlorate in wet deposition across North America. *Environ. Sci. Technol.* **43**, 616–622.

Rao B., Anderson T. A., Orris G. J., Rainwater K. A., Rajagopalan S., Sandvig R. M., Scanlon B. R., Stonestrom D. A., Walvoord M. A. and Jackson W. A. (2007) Widespread natural perchlorate in unsaturated zones of the southwest United States. *Environ. Sci. Technol.* **41**, 4522–4528.

Seyfferth A. L., Sturchio N. C. and Parker D. R. (2008) Is perchlorate metabolized or re-translocated within lettuce leaves?. A stable-isotope approach. *Environ. Sci. Technol.* **42**, 9437–9442.

Sherif M., Almulla M., Shetty A. and Chowdhury R. (2014) Analysis of rainfall, PMP, and drought in the United Arab Emirates. *Int. J. Climatol.* **34**, 1318–1328.

Sigman D. M., Casciotti K. L., Andreani M., Barford C., Galanter M. and Böhlke J. K. (2001) A bacterial method for the nitrogen isotopic analysis of nitrate in seawater and freshwater. *Anal. Chem.* **73**, 4145–4153.

Stern J. C., Sutter B., Freissinet C., Navarro-González R., McKay C. P., Archer P. D., Buch A., Brunner A., Coll P., Eigenbrode J., Fairen A., Franz H., Glavin D., Kashyap S., McAdam A., Ming D., Steel A., Szopa C., Wray J., Martin-Tores J., Zorzano M. and Conrad P.MSL Science Team (2015) Evidence for indigenous nitrogen in sedimentary and aeolian deposits from the Curiosity rover investigations at Gale crater, Mars. *Proc. Natl. Acad. Sci.*, www.pnas.org/cgi/doi/10.1073/pnas.1420932112.

Sturchio N. C., Caffee M., Beloso A. D., Heraty L. J., Böhlke J. K., Hatzinger P. B., Jackson W. A., Gu B., Heikoop J. M. and Dale M. (2009) Chlorine-36 as a tracer of perchlorate origin. *Environ. Sci. Technol.* **43**, 6934–6938.

Sturchio N. C., Böhlke J. K., Gu B., Hatzinger P. B. and Jackson W. A. (2011) Isotopic tracing of perchlorate in the environment: Chapter 22. In *Handbook of environmental isotope geochemistry* (ed. M. Baskaran). Springer-Verlag, pp. 437–452.

Tan K., Anderson T. A. and Jackson W. A. (2004a) Degradation kinetics of perchlorate in sediments and soils. *Water Air Soil Pollut.* **151**, 245–259.

Tan K., Anderson T. A., Jones J., Smith P. and Jackson W. A. (2004b) Accumulation of perchlorate in aquatic and terrestrial plants at a field scale. *J. Environ. Qual.* **33**, 1638–1646.

Tan K., Anderson T. and Jackson W. A. (2006) Uptake and exudation behavior of perchlorate in smartweed. *Int. J. Phytorem.* **8**(1), 13–25.

Van Aken B. and Schnoor J. L. (2002) Evidence of perchlorate (ClO_4^-) reduction in plant tissues (poplar tree) using radio-labeled $^{36}ClO_4^-$. *Environ. Sci. Technol.* **36**, 2783–2788.

Voogt W. and Jackson W. A. (2010) Perchlorate, nitrate, and iodine uptake and distribution in lettuce (*Lactuca sativa* L.) and potential impact on background levels in humans. *J. Agric. Food Chem.* **58**(23), 12192–12198.

Ye L., You H., Yao J., Kang X. and Tang L. (2013) Seasonal variation and factors influencing perchlorate in water, snow, soil and corns in Northeastern China. *Chemosphere* **90**, 2493–2498.

Associate editor: Jack J. Middelburg